minerals

MDPI

Review

^{210}Pb and ^{210}Po in Geological and Related Anthropogenic Materials: Implications for Their Mineralogical Distribution in Base Metal Ores

Nigel J. Cook [1,*], Kathy J. Ehrig [2], Mark Rollog [1], Cristiana L. Ciobanu [1], Daniel J. Lane [1], Danielle S. Schmandt [1], Nicholas D. Owen [1], Toby Hamilton [3] and Stephen R. Grano [4]

1 School of Chemical Engineering, The University of Adelaide, Adelaide, SA 5005, Australia; mark.rollog@adelaide.edu.au (M.R.); cristiana.ciobanu@adelaide.edu.au (C.L.C.); daniel.lane@adelaide.edu.au (D.J.L.), danielle.schmandt@adelaide.edu.au (D.S.S); nicholas.owen@adelaide.edu.au (N.D.O.)
2 BHP Olympic Dam, Adelaide, SA 5000, Australia; Kathy.J.Ehrig@bhpbilliton.com
3 School of Chemical Engineering, The University of Queensland, Brisbane, QLD 4072, Australia; t.hamilton1@uq.edu.au
4 Institute for Mineral and Energy Resources, The University of Adelaide, Adelaide, SA 5005, Australia; stephen.grano@adelaide.edu.au
* Correspondence: nigel.cook@adelaide.edu.au; Tel.: +61-8-8313-1096

Received: 19 April 2018; Accepted: 10 May 2018; Published: 13 May 2018

Abstract: The distributions of ^{210}Pb and ^{210}Po, short half-life products of ^{238}U decay, in geological and related anthropogenic materials are reviewed, with emphasis on their geochemical behaviours and likely mineral hosts. Concentrations of natural ^{210}Pb and ^{210}Po in igneous and related hydrothermal environments are governed by release from crustal reservoirs. ^{210}Po may undergo volatilisation, inducing disequilibrium in magmatic systems. In sedimentary environments (marine, lacustrine, deltaic and fluvial), as in soils, concentrations of ^{210}Pb and ^{210}Po are commonly derived from a combination of natural and anthropogenic sources. Enhanced concentrations of both radionuclides are reported in media from a variety of industrial operations, including uranium mill tailings, waste from phosphoric acid production, oil and gas exploitation and energy production from coals, as well as in residues from the mining and smelting of uranium-bearing copper ores. Although the mineral hosts of the two radionuclides in most solid media are readily defined as those containing parent ^{238}U and ^{226}Ra, their distributions in some hydrothermal U-bearing ores and the products of processing those ores are much less well constrained. Much of the present understanding of these radionuclides is based on indirect data rather than direct observation and potential hosts are likely to be diverse, with deportments depending on the local geochemical environment. Some predictions can nevertheless be made based on the geochemical properties of ^{210}Pb and ^{210}Po and those of the intermediate products of ^{238}U decay, including isotopes of Ra and Rn. Alongside all U-bearing minerals, the potential hosts of ^{210}Pb and ^{210}Po may include Pb-bearing chalcogenides such as galena, as well as a range of sulphates, carbonates, and Fe-oxides. ^{210}Pb and ^{210}Po are also likely to occur as nanoparticles adsorbed onto the surface of other minerals, such as clays, Fe-(hydr)oxides and possibly also carbonates. In rocks, unsupported ^{210}Pb- and/or ^{210}Po-bearing nanoparticles may also be present within micro-fractures in minerals and at the interfaces of mineral grains. Despite forming under very limited and special conditions, the local-scale isotopic disequilibrium they infer is highly relevant for understanding their distributions in mineralized rocks and processing products.

Keywords: ^{210}Pb; ^{210}Po; uranium decay chain; radionuclides; mineral deportment

1. Introduction

^{210}Pb and ^{210}Po are intermediate isotopes within the ^{238}U decay-series (Figure 1) and occur in minute amounts in nature [1]. Details of the uranium (^{238}U, ^{235}U) and thorium (^{232}Th) decay-series radionuclides are concisely provided in the review by Cowart and Burnett (1994) [2].

^{210}Pb has a half-life of 22.2 years and is generated via: (i) the decay of atmospheric ^{222}Rn gas ("unsupported" ^{210}Pb); and (ii) via the continuous production of ^{222}Rn from natural ^{226}Ra contained in crustal materials ("supported" ^{210}Pb). ^{210}Pb decays to ^{210}Bi by emission of a beta particle. ^{210}Pb is useful for determining the age of a recent sediment in that, provided that the atmospheric flux is constant, the decay profile relates directly to sedimentation rate. Hence, ^{210}Pb is useful for dating sediments up to a century or so old.

Polonium has no stable isotope [3,4]. ^{210}Po is by far the longest-lived of the 7 naturally-occurring Po isotopes in the U and Th decay-series (half-life = 138.376 days). ^{210}Po is generated via beta decay from ^{210}Bi (half-life 5.01 days) and decays to ^{206}Pb by emission of an alpha particle. It has a high specific activity (1.66×10^{14} Bq·g^{-1}) and is highly toxic [5] and one of the most radioactive natural radioisotopes; 1 mg of ^{210}Po emits as many alpha particles per second as 5 g ^{226}Ra. Its toxicity in nature is, however, limited by its vanishingly small mass concentration, even compared to ^{226}Ra. As an energy-generating alpha emitter, ^{210}Po has been used as a lightweight heat source to power thermoelectric cells, for example in the Russian Lunokhod lunar rovers to keep their internal components warm during the lunar nights. The principal source of both ^{210}Pb and ^{210}Po in the environment is natural ^{222}Rn gas which escapes to the atmosphere and undergoes radioactive decay. Airborne particles containing sorbed amounts of these highly particle-reactive decay products of ^{222}Rn fall to the land or water surface and either dissolve, are deposited onto soils, or become subject to sedimentation.

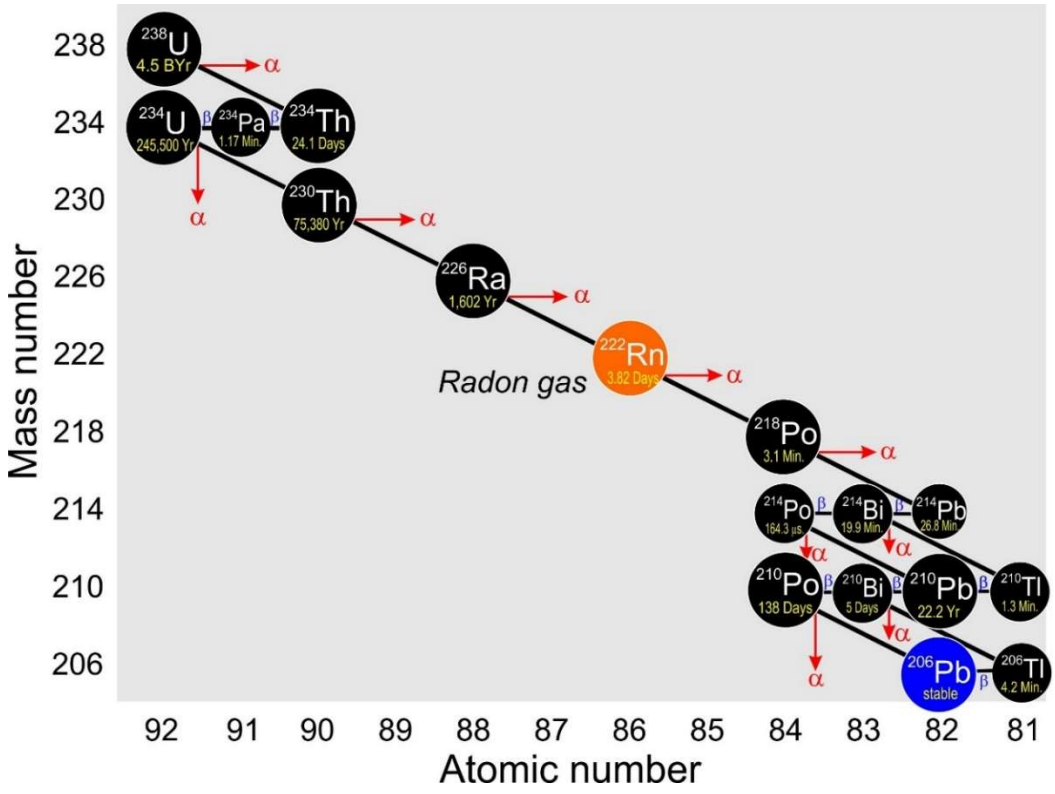

Figure 1. The uranium (radium series) decay chain, indicating half-lives, adapted from various publicly available sources.

Both radionuclides are, however, found in trace amounts in a range of solid media, both natural and anthropogenic in origin. ^{210}Pb and ^{210}Po are present in higher activity concentrations relative to crustal averages in uranium-bearing ores, and in the products of mining and processing from such deposits, including concentrates and wastes. While polonium concentrations are extremely low (< 0.1 mg/tonne even in high-grade uranium ores [6]), the presence of short half-life radionuclides (RN) can impact on the treatment, processing and transport of ore and resulting concentrates. In mining operations in which uranium is present, whether exploited or not, a knowledge of the geochemical behaviour of ^{210}Pb and ^{210}Po during mineral processing is critical to ensure that produced concentrates are as clean as possible. These radionuclides, whether occurring together with parent uranium in the mineralized rocks, or spatially decoupled from it as U-bearing minerals begin to break down, may represent a non-target element that could attract a financial penalty when sold on the open market. If present at high enough concentrations, saleability of that product may be prevented altogether (e.g., [7]). More extensive, and expensive, safety protocols and transport measures may also be required [8].

A comprehensive understanding of the geochemical behaviour and mineralogical distribution of ^{226}Ra, ^{210}Pb and ^{210}Po during ore processing is a pre-requisite for the development of methods to remove or reduce their concentration in products from minerals processing, and provides the motivation behind the present study. The following review of the distributions of ^{210}Pb and ^{210}Po (and of parent ^{226}Ra) in a broad range of geological materials builds on existing reviews of various length [9–12], many of which have emphasised the environmental and health risks that ^{210}Pb and ^{210}Po present. Our emphasis is on the concentrations and distributions of ^{210}Pb and ^{210}Po in solid media, with focus on mineralized rocks and ores, and in anthropogenic materials resulting from the exploitation of natural resources. An assessment of the likely mineral hosts for both ^{210}Pb and ^{210}Po in critical geological environments, including ores and in non-nuclear industrial sources (technologically enhanced naturally occurring radionuclide material (TENORM; [11]) follows.

2. Crustal Distribution of ^{210}Pb and ^{210}Po

^{210}Pb and ^{210}Po are widely dispersed in a large variety of natural media because they often mimic the distributions of parental ^{238}U, ^{226}Ra, or ^{222}Rn. Much of the literature on ^{210}Pb and ^{210}Po distributions in nature is focused on their concentrations in the atmosphere (e.g., [13]), in oceans (e.g., [14–17]), rivers (e.g., [18]), lakes (e.g., [19]), groundwaters (e.g., [20–23]), drinking waters (e.g., [24–26]), and soils [27–29]. Attention has also been given to mosses and lichens, which efficiently capture atmospheric ^{210}Pb and ^{210}Po, peat bogs (also anomalous with respect to ^{210}Pb and ^{210}Po), and in the animal and human food chains, e.g., milk or berries, and particularly seafood (e.g., [12,30–32]). A smaller body of data is available for some natural environments, notably hydrothermal ore deposits or active volcanic fumaroles, where there is evidence for the selective fractionation of ^{210}Pb and ^{210}Po from other ^{238}U decay products, and where ^{210}Pb and ^{210}Po are concentrated in "new" precipitates. These particle-sensitive decay product isotopes are always fractionated from gaseous parent ^{222}Rn that has extreme dispersion and mobility in the environment, particularly in the atmosphere.

There is a large body of data addressing the distribution and behaviour of ^{210}Pb and ^{210}Po in both magmatic and marine/lacustrine sedimentary environments, as well as in relation to the mining, processing and smelting of uranium-bearing ores, processing of phosphate ores for phosphoric acid production and other human activity. Somewhat less well documented are concentrations of ^{226}Ra, ^{210}Pb and ^{210}Po in other anthropogenic materials such as coal ash (e.g., [33,34]), and as scales and sludges associated with oil and gas production [35–37]. Not infrequently, observed distributions are the product of a complex interplay between natural and anthropogenic ^{226}Ra, ^{210}Pb and ^{210}Po from different mining and non-mining sources, the effects of which can only be elucidated by high-quality analysis and a good understanding of the physical and historical context of the samples in question (e.g., [38,39]). There is generally a strong link between the distributions of ^{210}Pb and ^{210}Po and that of parent ^{226}Ra in many industrial wastes (uranium mill tailings, phosphogypsum, coal fly ash, oilfield

scales and sludges) such that understanding the mode-of-occurrence of ^{226}Ra will enable prediction of ^{210}Pb and ^{210}Po behaviour. There are, however, some exceptions in which selective fractionation and concentration of ^{210}Pb and ^{210}Po takes place, as will be shown below.

A detailed treatment of analytical techniques for the determination of short-lived isotopes at concentrations of small fractions of parts-per-billion, and quantification of ^{210}Pb and ^{210}Po in rocks, minerals, concentrates and leachates, lie beyond the scope of this contribution. The reader is referred to References [1,40,41], in which comprehensive reviews of methodologies used for the determination of ^{210}Po in environmental materials are provided, building on earlier studies [42] and others. Clayton and Bradley (1995) [43] describe their methodology to measure ^{210}Pb and ^{210}Po in a range of environmental materials. In a series of papers, Jia and co-authors [44–46] have put forward procedures for analysis of ^{210}Pb and ^{210}Po in mineral, biological and soil samples. Particularly relevant to our focus on ^{210}Pb and ^{210}Po distributions in ores and ore processing residues are separation techniques outlined by Prud'homme et al. (1999) [47] for fine-grained multi-phase materials.

2.1. Magmatic Rocks and Related Hydrothermal Systems

Volcanoes represent the largest single contributor of atmospheric ^{210}Pb and ^{210}Po. For example, Allard et al. [48] document extremely high fluxes from the Ambrym basaltic volcano, Vanuatu Island Arc, in the South Pacific Ocean. Based on direct measurements, these authors maintain that this volcano is among the most powerful volcanic gas emitters on Earth, producing between 5% and 9% of current estimates for global subaerial volcanic emissions of ^{210}Pb and ^{210}Po. Data for both dissolved and emitted magmatic volatiles are used to estimate the depth, size and degassing rate of the basaltic magma reservoir that sustains the eruptive activity [48]. In the aforementioned paper, Allard et al. note radioactive disequilibrium of ^{210}Pb, ^{210}Bi and ^{210}Po in the volcanic gas phase and use this to constrain the renewal rate and dynamic time scales of the magma reservoir. Extensive radioactive disequilibrium between the three radionuclides reported in Ambrym volcanic gas is concordant with observations from other basaltic volcanoes [49,50]. The radioisotopic disequilibrium is attributed by Allard et al. [48] to the very different volatilisation rates of the three radionuclides during high-temperature basalt degassing (^{210}Po > ^{210}Bi > ^{210}Pb). All ^{210}Po is volatilised, whereas the emanation rate is two orders of magnitude lower. ^{210}Po–^{210}Pb geochronology is routinely used to date recent volcanic eruptions (e.g., [51]). Measurable activity of ^{210}Pb, ^{210}Bi and ^{210}Po is not restricted to basaltic volcanoes. The volatility of all three radionuclides have been studied in andesitic gases from Merapi Volcano, Indonesia [52], although the authors note that the emanation coefficients are significantly lower than observed at basaltic volcanoes, a feature attributed to lower magma temperatures. The same authors state that the radionuclides are mainly transported in the volcanic gases as Pb-chlorides, and as "Bi- and Po-metallic species".

The radionuclide systematics of igneous activity nevertheless differ considerably with respect to tectonic environments [53]. Enrichment of ^{210}Po and ^{226}Ra relative to ^{230}Th is noted to be more common and greater in island arcs than in continental margin subduction environments. Levels of enrichment tend to decrease with differentiation. Differences were attributed [53] to variations in the process of melt extraction, changes in bulk partition coefficients within the mantle wedge, or preferential addition of U from subducted lithosphere.

Interest in the activity of ^{210}Pb and relationships with parent radionuclides in young volcanic rocks centres on the useful geochronological information the radioisotope distributions can provide. The literature reveals substantial debate about the possible causes of observed isotopic disequilibria in many young volcanic rocks (e.g., [54]). The observed ^{210}Pb deficits relative to ^{226}Ra are attributed to magma degassing over decades rather than partial melting or interaction with cumulates [55].

Most igneous rocks contain both U and Th, with concentrations increasing as silica content increases. Granites are thus the rock type with the highest concentration of all daughter radionuclides, which remain in secular equilibrium until weathered. Uranium, Th and daughter radionuclides are important heat producers in granitic rocks [56].

Radionuclide concentrations have been examined in volcanic fumaroles from La Fossa cone, Vulcano Island, Italy [57,58]. Sulphur and sulphide incrustations show relative but variable enrichments in ^{210}Po (as high as 500 Bq·g^{-1}), and in ^{210}Pb relative to ^{226}Ra, which are related to degassing of the fumarolic fluids. The published data record mobility of sublimates within the fumaroles. ^{210}Po is almost fully volatilised due to the relatively high velocity of the gas, even though temperatures did not exceed 280–350 °C. Much ^{210}Po may therefore be present in gaseous form within the fumarole. Sublimates at La Fossa Crater, Aeolian Islands, Italy [59] contain an abundance of rare Pb–Bi-sulphosalt mineral species (e.g., wittite, cannizzarite, mozgovaite, etc. [60,61]). Several of sulphosalts, including Cl- and Br-bearing species (e.g., vurroite [62]) have been first described from the locality.

The unusually high sulphur-reducing environments offered by deep-sea hydrothermal vents display ^{210}Pb and ^{210}Po enrichment relative to ^{226}Ra. Boisson et al. (2001) [63], for example, describe the relative enrichment in naturally-occurring ^{210}Po and ^{210}Pb associated with the high particle fluxes brought about by hydrothermal venting off the island of Milos, Aegean Sea. ^{210}Po levels in organisms living on or near the microbial mat in the vent zone were higher than from non-vent areas. It was, however, stressed [63] that input of ^{210}Po and ^{210}Pb to oceans through venting activity is probably not significant compared to that of atmospheric origin. High levels of natural radioactivity, including ^{210}Po–^{210}Pb, in vent biota from both the East Pacific Rise and Mid-Atlantic Ridge have been confirmed [64].

2.2. Sedimentary Environments

Measurable concentrations of ^{210}Pb and ^{210}Po in sedimentary environments, whether marine, lacustrine, deltaic or fluvial have proven invaluable for understanding age relationships of sediments on the decade-scale and for calculation of rates of sedimentation. Many dozens of case studies, e.g., [65–68], document the spatial distributions of ^{210}Pb and ^{210}Po, and successfully separate natural from anthropogenic sources. Activities of ^{210}Pb and ^{210}Po have also proven valuable for studies of glaciation and the accumulation and melting rates of ice sheets [69]. Remarkably few of these studies have addressed the mineralogy of the sediments, and the likely host(s) of ^{210}Pb and ^{210}Po.

A key feature of many studies of sediments and water columns in marine or lake waters is the recognition of disequilibrium between ^{210}Pb and ^{210}Po that is linked to differential cycling patterns, rates of sequestration by sediments, as well as the contributions of atmospheric deposition, particularly for ^{210}Po.

Some sedimentary rocks contain anomalous radionuclide concentrations. Of particular note are restricted marine and estuary environments supplied by organic- and clay-rich sediment. Under reducing conditions, uranium is readily adsorbed onto the organics and/or clay particles.

Sedimentary rocks are also the host for many of the World's largest and richest uranium deposits, formed via migration of dissolved U^{6+} in oxidising waters along paleoaquifers and deposited in reduced rocks. The genesis of such deposits has been amply described elsewhere [70].

3. ^{210}Pb and ^{210}Po from Anthropogenic Sources

The mining of uranium, smelting of copper and polymetallic ores, phosphoric acid and oil/gas production and combustion of coal (and peat) are the main extractive activities leading to generation of materials with high contents of ^{210}Pb, ^{210}Po, and other RN. Surveys of the generation of Naturally Occurring Radioactive Materials (NORM) from industrial operations [71–75] also cover other industrial sectors, including manufacture of zirconia, titanium dioxide pigment production, cement production and alumina and iron and steel production.

3.1. ^{210}Pb and ^{210}Po in Uranium Mill Tailings

The radiological risks associated with management of uranium mill tailings have been discussed by [76–79], among many others. Several authors have suggested that ^{226}Ra occurs in radium-bearing sulphate minerals in uranium mill tailings [80–82]. Landa et al. [83] examined uranium mill tailings from Monticello, Utah. ^{226}Ra was found to be associated with particles and colloids of alkaline-earth sulphates, alkaline-earth carbonates, and surfaces of quartz, clay, and feldspar. Landa [77] inferred from the leaching behaviour of uranium mill tailings that ^{226}Ra occurs with hydrous oxides of iron and manganese. In one study specially aimed at understanding the mineralogy of ^{210}Po [84], material from three uranium mill sites in the USA were examined to establish where contaminants reside as a prerequisite for modelling contaminant mobilisation. Four mineral hosts were suggested using a combination of electron probe microanalysis, thin-section petrography, α-emission mapping, and selective chemical extractions (although none of these techniques can identify mineral hosts for specific radioactive decay products): uranium minerals, authigenic siliceous material, Ba–Sr-sulphates, and Fe–Ti–V-oxides. These themes are explored further by Landa and Bush [79], who recognised a redistribution of radium by particle size during milling but also of the components in the tailings onto which radionuclides are adsorbed. The following potential sorbents were identified: clay minerals, Fe- and Al-oxides, feldspars, fluorite, barite, jarosite, coal, and volcanic glass. Both ^{226}Ra and ^{210}Pb showed both higher degrees of adsorption than either ^{238}U or ^{230}Th, attributable to either selective adsorption or ingrowth of ^{210}Pb daughter isotopes in minerals containing substituted radium (e.g., Ra^{2+} for Ca^{2+}).

In a review of the mineralogical controls on radionuclide mobility in uranium mill tailings [78], the importance of amorphous silica, carbonates and phosphates, and microbial reduction processes is noted. The same publication also examines radionuclide behaviour (although not mentioning ^{210}Pb and ^{210}Po in this context) during in-situ leach (ISL) recovery operations. Jarosite [$KFe_3(SO_4)_2(OH)_6$], which may precipitate and severely restrict permeability along ISL aquifers, is said to be a significant host for radium. The presence of sulphides and Fe-(hydr)oxides will also impact on recovery dependent on the extracting agent used. These ideas are expanded in a more recent study of uranium mill tailings [85] that also stresses the potential role of sulphates and secondary galena as hosts for ^{210}Pb. It is reasonable to infer that these minerals scavenge ^{210}Pb dissolved within pore fluids.

Radionuclide distributions, including ^{210}Pb deposition rates and inventories, have been examined in and around the Ranger Uranium Mine, N.T., Australia [86]. Natural redistributions of ^{222}Rn and ^{210}Pb occur via atmospheric dispersion of ^{222}Rn, (seasonal) deposition of ^{210}Pb on surfaces, and eventual migration creating ^{210}Pb depth profiles prior to decay to ^{206}Pb. A net loss of ^{210}Pb from the region occurs during the dry season by attachment to aerosols.

3.2. ^{210}Pb and ^{210}Po in Copper and Polymetallic Ores and Products of Their Mining and Processing

Some copper ores contain anomalously high concentrations of RN, meaning that daughter radionuclides are present in products of mining and smelting, and within wastes resulting from those activities. Due to selective volatilization/condensation of ^{210}Pb and ^{210}Po, smelter dusts tend to be enriched in ^{210}Pb and ^{210}Po compared to ^{226}Ra, compared to their activity concentrations in the original ore feed, and compared to their activity concentrations in other solids produced during processing. Such a scenario is documented for the Olympic Dam copper mining and smelting operation, South Australia [87]. The behaviour of ^{210}Pb and ^{210}Po during concentration and smelting of copper ores, and their preferential partitioning into smelter flue dusts where they may accumulate, has been documented in several studies. One of the best studied examples is the contamination generated through centuries of exploitation of copper-bearing bituminous shales (Kupferschiefer) in the Mansfeld district of eastern Germany. A characterisation of scrubber dust slurries (*Theisenschlamm*) containing ^{210}Pb and ^{210}Po, which were produced as a by-product of the Mansfeld smelting operations, is given in [88]. Around 220,000 tonnes of these sludges are deposited at several sites and continue to represent a serious environmental risk [89–92]. The material contains: 18% Zn (as sphalerite and wurtzite);

14% Pb (as galena and secondary anglesite); a wide variety of hazardous (As, Tl, Cd) elements and rare metals (Ag, Ge, Re); polycyclic aromatic hydrocarbons and other organic compounds, as well as radionuclides. ^{210}Pb and ^{210}Po are concentrated in the finest size fractions, typically of sub-micron size and combined as aggregates with mean diameter of 1.25 µm [88]. Additional characterisation of the *Theisenschlamm* is provided by Morency et al. [93], with experimental evidence in support of oxidative processes designed to immobilize elements and isotopes of concern. Of relevance to the overarching aim of the present study is the observation that almost all ^{210}Pb and ^{210}Po can be concentrated into a lead sulphate phase. Ores of comparable age and origin, albeit with generally lower associated radioactivity, are currently mined in the Lubin region, Poland [94]. The highly selective enrichment of ^{210}Pb and ^{210}Po compared to ^{226}Ra in certain wastes from copper smelting highlights the importance of understanding the distribution of these isotopes when designing plant operations or planning waste clean-up or handling.

Hypogene tin ores are generally genetically related to granites and often contain anomalous concentrations of Cu, Pb, Bi, U and Te relative to crustal averages. They may contain measurable concentrations of ^{210}Pb, ^{210}Po and ^{210}Bi. The smelter process, for which feedstock may not only comprise tin ores/concentrates but also tin-rich residues from other processes, involves a molten metal stream and separation into tin, lead and lead-bismuth alloys. ^{210}Po will rapidly volatilise, and according to Martin et al. [71], can be highly enriched in smelter fumes (200,000 Bq·kg^{-1}). Slags will contain the non-volatile radionuclides but also some ^{210}Pb and ^{210}Po (10,000 Bq·kg^{-1}). Within the bismuth metal, short-lived ^{210}Bi rapidly decays to ^{210}Pb, which may have activity concentrations up to 100,000 Bq·kg^{-1}. Hipkin and Paynter (1991) [95] address activity concentrations of materials and the radiation exposures of workers in the tin industries of Bolivia and SE Asia, while background data on ^{210}Pb and ^{210}Po behaviour during the tin smelting and electro-refining process are given by Harvey et al. [96]. ^{210}Pb and ^{210}Po activities in and around a large, now-closed, tin smelter in northern England are discussed by Baxter et al. [97]. Here, over the course of ca. 55 years of tin production, about 30% of the ^{210}Po was isolated in tellurium dross, 48% decayed within the refinery, 19% went to waste slag, and 2% was released into the atmosphere.

3.3. ^{210}Pb and ^{210}Po in Mining and Processing of Phosphates

Many phosphate formations exploited for the fertiliser industry contain concentrations of naturally occurring radionuclides of the uranium and thorium decay series that exceed those in other rocks. The risks associated with mining, milling and manufacturing of phosphoric acid and phosphate fertilizers have been widely documented at different sites around the world. Solid waste products of the phosphate industry, notably gypsum ($CaSO_4 \cdot 2H_2O$), termed phosphogypsum, but also dusts generated during milling, can carry particularly high concentrations of ^{226}Rn, ^{210}Pb and ^{210}Po (e.g., [74,98–109]. Although waste from the phosphate industry has, in some cases, been disposed of in the marine environment (e.g., [101]), elsewhere, most spectacularly in Florida, where the World's largest phosphoric acid industry is centred, huge waste piles (gypstacks) have been generated, creating serious waste management issues.

In the manufacture of phosphoric acid, an important industrial chemical, phosphate rock (which typically contains U within apatite or other phosphates) is treated with sulphuric acid, resulting in by-product gypsum in volumes three times greater than the phosphoric acid (Figure 2). The reaction involved in phosphoric acid production can be simplified, after Burnett et al. [103], as:

$$Ca_{10}(PO_4)_6F_2 + 10H_2SO_4 + 20H_2O \rightarrow 10CaSO_4 \cdot 2H_2O + 6H_3PO_4 + 2HF$$

The above reaction creates disequilibrium between U, Th and Ra. The majority of U if found in the phosphoric acid, ca. 90% of the ^{226}Ra, and effectively all the ^{210}Pb and ^{210}Po, will be preferentially concentrated within the phosphogypsum (e.g., [110]), with ^{210}Pb and ^{210}Po in secular equilibrium [111]. The ^{210}Pb and ^{210}Po activities in phosphogypsum are typically a few hundreds of Bq·kg^{-1}. For example,

Brasilian phosphogypsum described by Mazzilli et al. [106] shows concentration ranges of 47–894 $Bq \cdot kg^{-1}$ and 53–677 $Bq \cdot kg^{-1}$ for ^{210}Pb and ^{210}Po, respectively. These activities depend on the uranium concentrations in the phosphate ore, which can vary over as much as an order of magnitude. For comparison, phosphate rocks in Florida, Morocco and Jordan, three important producing areas, contain 1300–1850 $Bq \cdot kg^{-1}$ U [112]. In the phosphate rocks, U (and Th) is present mostly within the mineral apatite. U^{4+} has a similar ionic radius to Ca^{2+} (0.97 and 0.99 Å, respectively) and readily substitutes into the apatite lattice, resulting in less abundant uraninite in some ores.

The physical distribution of ^{226}Ra and ^{210}Pb in phosphogypsum waste piles is addressed by Rutherford et al. [100], who note heterogeneity in which ^{210}Pb is concentrated in the finest fraction (no more than a few microns). In studies of Florida phosphogypsum, $^{210}Pb/^{210}Po$ disequilibrium in mature phosphogypsum samples has been demonstrated [104], suggesting that ^{210}Pb was more mobile than either ^{210}Po or ^{226}Ra. Although none of the phosphogypsum research has demonstrated that the mineral hosts for each radionuclide differ (phosphogypsum is, in any case essentially monomineralic with around 1% impurities), these observations are indirect evidence to the suggestion that ^{210}Pb may be less well bound within the crystal lattice of gypsum.

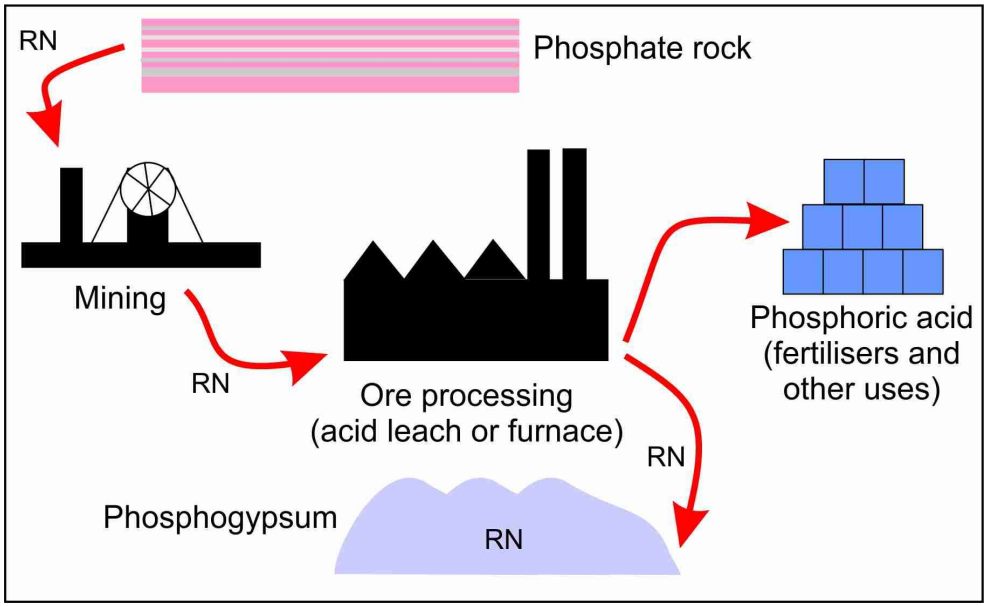

Figure 2. Schematic diagram showing RN behaviour during phosphate production.

3.4. ^{210}Pb and ^{210}Po Associated with Oil and Gas Production

Radioactive scales and sludges associated with offshore oil and gas production often contain anomalously high concentrations of ^{226}Ra, ^{210}Pb and ^{210}Po, and have been well documented [35–37,113,114]. After the mixture of oil, gas and water is brought to the surface, and the gas and formation waters are separated from the oil, hard scales will build up on the internal surfaces of the oil field extraction and production equipment. Well fluids (saline formation waters that are co-produced with oil and gas and require separate handling) are characteristically enriched in Ca, Sr, Ba and associated Ra. Pipes and tanks that come into contact with these waters are subject to scale and sludge build-up. The relative amounts of solid waste (sludges and sands) vary with the production area due to the different geological and fluid characteristics of the reservoirs. ^{226}Ra, ^{210}Pb and ^{210}Po-enriched scales precipitate as solids directly from the formation waters following changes in temperature, pressure and salinity.

The volumes of these materials are, however, generally rather small and typically comprise a mixture of carbonate and sulphate compounds of calcium, strontium and barium. Generation of ^{210}Pb and ^{210}Po is due to the presence of parent U and Th in the oil/gas source rocks, which decays to Ra that dissolves within the saline formation waters that also contain P, Sr, Ba and Ca. The radium isotopes, ^{226}Ra and ^{228}Ra, co-precipitate with the salts of these elements, enriching the sludges and, particularly, scales in radium and products of radium decay, including radon isotopes, ^{210}Pb and ^{210}Po. The relatively longer-lived decay products such as ^{210}Pb, will accumulate as very thin films and deposits in gas handling equipment and storage tanks.

3.5. ^{210}Pb and ^{210}Po from Combustion of Coal and Other Solid Fuels

The combustion of solid fuels such as coal for heat and power applications is an important source of atmospheric ^{210}Pb and ^{210}Po and has been studied in detail in various parts of the World. During the combustion of solid fuels, trace elements, including ^{210}Pb and ^{210}Po, partially volatilise along with organic constituents in the fuel matrix. The remaining trace elements remain in the fuel bed and are eventually collected as bottom ash. The volatilised fraction generally condenses on fly ash particles in the flue gases as the flue gases are cooled [115]. Fly ash samples collected from coal-fired power stations have been reported to contain elevated concentrations of ^{210}Pb and ^{210}Po, when compared with the original feedstocks [116], indicating that these two radionuclides volatilise to a large extent during the combustion of solid fuels. The United Nations Scientific Committee on the Effects of Atomic Radiation (UNSCEAR) provide further evidence for the enrichment of ^{210}Pb and ^{210}Po relative to precursor RN in fly ashes during solid fuel combustion in their survey on the activity concentrations of radionuclides in coal samples sourced from a wide range of geographical locations and in fly ashes sourced from various coal-fired power stations [117]. Country-averaged activity concentrations for coal were all within 50 Bq·kg^{-1} for both ^{210}Pb and ^{210}Po. Average concentrations of ^{210}Pb and ^{210}Po in the fly ash samples were much higher by comparison (930 Bq·kg^{-1} for ^{210}Pb and 1700 Bq·kg^{-1} for ^{210}Po). Studies on the size distribution of radionuclides in fly ash show ^{210}Pb and ^{210}Po to preferentially condense on fine particles below 10 microns in size [118,119]. This makes the capture of ^{210}Pb and ^{210}Po difficult, since conventional particulate control devices (e.g., electrostatic precipitators and bag filters) generally become less effective with diminishing particle size [119]. Consequently, a small but nevertheless not insignificant fraction of the ^{210}Pb and ^{210}Po in solid fuels is emitted from the stack into the atmosphere. According to Roeck et al. [120], in old coal-fired power plants, ca. 3% of the initial radioactivity will be discharged from the stack but this proportion is no more than 0.5% in modern plants. UNSCEAR [121] state that annual emissions from a "typical" 600 MW coal fired power station was 0.4 GBq for ^{210}Pb and 0.8 GBq for ^{210}Pb. ^{210}Pb and ^{210}Po may also accumulate in deposits on furnace walls and on the fireside of boiler tubes.

The amounts of ^{210}Pb and ^{210}Po released into the different product streams during solid fuel combustion not only depend on processing parameters (e.g., combustion temperature and gas atmosphere) but also on the properties of the feedstock, particularly the activity concentrations of ^{210}Pb and ^{210}Po. Most coals contain small amounts of parent U and Th but their concentrations can vary over several orders of magnitude from deposit to deposit. There is a substantial volume of literature on naturally occurring radionuclide distributions in coals and fly ash [116,122–125]. Coal is formed via reduction of organic material, in which uranium is trapped or adsorbed onto clay particles, carbonaceous matter, pyrite and organic matter. In contrast, Th occurs within minerals such as monazite or apatite. Since organic matter is an effective reductant, coal horizons may accumulate additional uranium over time by extracting dissolved uranium from circulating groundwaters [126]. Lower rank sub-bituminous coals, brown coals, and lignites may contain higher concentrations of parent U and Th ([125] and references therein). Unconsolidated analogues, including peats, may also contain anomalous RN concentrations.

Enhanced atmospheric ^{210}Po in urban areas may be attributed to coal-fired power stations [127,128]. In a comparison of emissions from power plants fuelled by different hydrocarbon fuels, Häsänen et al. [129] point out that the greatest emissions of ^{210}Po per burnt volume of fuel were from combustion of peat.

3.6. ^{210}Pb and ^{210}Po from Exploitation of Mineral Sands

Anomalous concentrations of ^{210}Pb and ^{210}Po are associated with exploitation of mineral sands for production of zircon and zirconia, titanium dioxide and rare earth elements. Radiological risks associated with such ores (and corresponding products and wastes) are generally low (around 10,000 Bq·kg^{-1} [71]). This could, however, be an area in which ^{210}Pb and ^{210}Po release is set to increase, since demand for these commodities, especially REE, is booming, and new mineral sands operations are being established around the globe.

Mineral sands are of particular interest because of the indirect information they provide on potential mineral hosts for ^{210}Pb and ^{210}Po. The minerals within such sands (zircon, baddeleyite, monazite, xenotime, ilmenite, rutile, etc.) all host trace to minor amounts of uranium and thorium (varying up to as much as 1 wt % depending on primary source) and are all highly refractory. Despite this, there are relatively few published studies detailing ^{210}Pb and ^{210}Po geochemistry in mineral sands enabling an understanding of whether daughter radionuclides are retained in the crystal structures. The manufacture of zirconia for glazes and ceramics involves production of small volumes (~1% of feed) of highly RN-enriched waste, as well as volatilisation of ^{210}Pb and ^{210}Po.

Titanium oxide pigment production, from rutile, a mineral that also commonly contains primary minor U and Th, also results in a RN-enriched solid waste residue.

3.7. ^{210}Pb and ^{210}Po in Other Anthropogenic Materials

Most iron ores contain only low concentrations of ^{210}Pb and ^{210}Po and thus accumulation of radioactivity in waste materials produced by iron and steel production are mostly attributable to other feed materials (coal/coke and limestone). ^{210}Pb and ^{210}Po tend to accumulate in the sinter plant in dust collected from the gas cleaning systems and are generally very low or absent in saleable products. According to Martin et al. [71], for every million tonnes of steel produced, 2000 tonnes of contaminated dust will be generated. In a study of sinter plant radioactivity in the Port Kembla foundry, NSW, Australia, Brown et al., in a report cited by Martin et al. [71], report activities of 18,900 and 15,600 Bq·kg^{-1} for ^{210}Pb and ^{210}Po, respectively, in ductwork dust.

Production of the elements niobium and tantalum is also associated with generation of RN-rich residues. Like tin ores, Nb–Ta ores are granite-related and commonly contain minor amounts of other elements including uranium (and thorium). Pyrochlore, a primary ore mineral of niobium and tantalum, will often contain actinides at measurable concentrations. ^{210}Pb activities as high as 16,700 Bq·kg^{-1} in slags from a Brasilian niobium processing facility are reported [11].

Martin et al. (1997) [71] compiled information on ^{210}Pb and ^{210}Po in cement, bricks and other building materials, and provide activity concentrations for ^{226}Ra and ^{232}Th. They note that activities are only of concern if substantial amounts of waste materials in which ^{210}Pb and ^{210}Po are concentrated are added into the materials. Examples include the common addition of copper slag in concrete (in the former East Germany), phosphogypsum waste in wallboard and road construction, and fly-ash in bricks and some cements. Lightweight building blocks may contain both slag and fly-ash. Several publications detail representative ^{210}Pb and ^{210}Po activity concentration data for building materials, focussing on eastern European countries where the practice of adding smelter slags and fly-ash was commonplace [130–132]. The environmental impact of radionuclide release during processing of granite rock for ornamental stone has also been explored [133]. In this paper, Guillén et al. suggest that even basic mechanical processing of granites can lead to increased levels of ^{210}Po and ^{210}Pb in the surrounding environment, as dusts, solid waste and slurries.

Numerous studies have sought to demonstrate the impact of historical human industrial activity by monitoring the levels of lead isotopes in peat bogs, salt marsh, lakes and estuarine sediments [38,134–140].

4. Mineral Repositories for ^{210}Pb and ^{210}Po

The literature contains extensive reference to the potential mineral repositories for ^{210}Pb and ^{210}Po, although much of this evidence has been obtained indirectly. Very few studies to date have been able to provide direct confirmation that a given phase contains these RN. This is largely due to those RN with relatively short half-lives being present at minute concentrations well below minimum detection limits of conventional microanalysis.

Polonium has no non-radioactive isotope and does not occur naturally as a metal or essential component of naturally occurring compounds, although the compound PbPo has been reported [141] and has been attributed to natural alpha decay of polonium to form lead. Polonium is readily vaporised, forming Po_2 molecules even well below the melting and boiling points (254 and 962 °C, respectively) via small clusters of polonium atoms spalled off by alpha decay. These particles are readily adsorbed. Chemically, polonium displays similar behaviour to that of tellurium and bismuth [141,142]. More than 50 polonium compounds have been synthesized including metal polonides, polonium hydride, the two oxides PoO_2 and PoO_3, halides and sulphates. Various oxidation states, including $^{2+}$, $^{4+}$ and $^{2-}$, are known.

Valuable insights into the behaviour of ^{210}Pb and ^{210}Po in polymetallic ores are provided by Golubev et al. [143]. By comparative analysis of different volumes of ore within a single vein-type uranium orebody, these authors provide critical evidence for migration of ^{238}U and, critically, of intermediate decay products within an effectively open system, creating disturbances of U–Pb systematics, expressed as local enrichments or depletions in ^{206}Pb, giving rise to discrepancies between ages based on ^{206}Pb/^{238}U and ^{207}Pb/^{235}U ratios. The authors note the presence of zones with low U contents but with excess ^{206}Pb. These contain pyrite/marcasite onto which migrating longer-lived radionuclides, including ^{210}Po and ^{210}Pb, are considered to accumulate, effectively playing the role of geochemical barriers within the system.

In a study attempting to identify the solid-phase partitioning of ^{210}Po and ^{210}Pb in anoxic marine sediments [144], the influence of early diagenetic processes on distribution patterns is documented. In sediment, ^{210}Po was found to be either bound to organic matter, sulphides such as pyrite, clay minerals or refractory oxides. ^{210}Po was found not to be significantly bound to acid volatile sulphides in sediment, even if the authors considered that ^{210}Po initially bound to acid volatile sulphides may have been redistributed by bioturbation.

Because of the extremely low concentrations and the difficulty of separating fine-grained minerals, there is a paucity of published concentration data for ^{210}Pb and ^{210}Po in individual minerals. Identification of the potential mineral repositories for either radionuclide, except for post-decay reincorporation of daughter RN into parent U-minerals is therefore reliant on indirect observation. Good indications as to potential hosts can nevertheless be made based on the literature we have summarised above (Table 1).

Table 1. Summary of potential mineral hosts for ^{210}Pb and ^{210}Po.

Mineral Group	Mineral	Formula (e)	Host for
Uranium minerals	Uraninite	UO_2 (ideally)	U, radiogenic Pb, minor Th
	Coffinite	$U(SiO_4)_{1-x}(OH)_{4x}$	ditto -
	Brannerite	$(U,Ca,REE)(Ti,Fe)_2O_6$	ditto -
	Uranothorite	$(Th,U)SiO_4$	Th, U, radiogenic Pb
	Carnotite	$K_2(UO_2)_2(VO_4)_2{\cdot}3H_2O$	U, (Th and Pb?)
REE-, Zr- and Nb–Ta-minerals	Monazite	$(REE)PO_4$	Minor U, Th radiogenic Pb?)
	Bastnäsite	$REE(CO_3)F$	ditto -
	Synchysite	$Ca(REE)(CO_3)_2F$	ditto -
	Xenotime	$(Y,REE)PO_4$	ditto -
	Alunite Supergroup Minerals (especially crandallite and beudantite groups)	(Various minerals)	ditto -
	Baddeleyite	ZrO_2	ditto -
	Zircon	$ZrSiO_4$	ditto -
	Tantalite-(Fe)–tantalite-(Mn) series	$(Fe,Mn,Mg)(Nb,Ta)_2O_6$	Trace U,Th,Pb (?)
	Euxinite	$(Y,Ca,Ce,U,Th)(Nb,Ta,Ti)_2O_6$	ditto -
Sulphides/selenides/tellurides	Galena	PbS	Radiogenic Pb
	Clausthalite	PbSe	ditto -
	Altaite	PbTe	ditto -
	Bi-chalcogenides	$Bi_x(Te,Se,S)_y$	?
	Pb-Bi-sulphosalts	(various)	?
	Pyrite	FeS_2	as a sorbent (?)
Carbonates	Calcite, dolomite, ankerite	$CaCO_3$, $CaMg(CO_3)_2$, $Ca(Fe,Mg)(CO_3)_2$	Ra, minor Pb
	Strontianite	$SrCO_3$	ditto -
	Rhodocrosite	$MnCO_3$	ditto -
	Magnesite	$MgCO_3$	ditto -
	Witherite	$PbCO_3$	Pb
Sulphates	Barite	$BaSO_4$	Ra, Pb
	Celestite	$SrSO_4$	ditto -
	Anglesite	$PbSO_4$	Pb
	Gypsum	$CaSO_4{\cdot}2H_2O$	Pb (?)
Fe-oxides, hydroxides	Hematite	α-Fe_2O_3	Minor/trace U, Pb, and as sorbent
	Goethite	FeO(OH)	As sorbent
Fe–Ti-oxides, Ti-oxides	Ilmenite	$FeTiO_3$	Minor U and Th
	Rutile	TiO_2	ditto -
Jarosite sub-group	Jarosite	$KFe(SO_4)_2(OH)_6$	Pb?
Other potential hosts	Apatite group	$Ca_5(PO_4)_3(F,Cl,OH)$	Minor U and Th
	Fluorite	CaF_2	?
	Feldspar group	-	Pb (replacing Ca?)

4.1. Re-Incorporation of Radionuclides into Parent Minerals

All minerals originally containing uranium will host daughter RN if those products do not migrate from the parent. Plausible ^{210}Pb and ^{210}Po carriers thus include the more common uranium minerals, such as uraninite, coffinite, uranothorite and brannerite, as well as the large number of minerals which carry trace to minor amounts of uranium. The latter include REE-fluorocarbonates and phosphates (monazite, bastnäsite, synchysite, florencite, xenotime, etc.), and common accessory minerals in rocks and ores such as apatite, allanite, zircon, titanite and rutile). The assumption that ^{210}Pb and ^{210}Po can be found in these minerals, however, infers that all decay chain products, including ^{234}Th, ^{226}Ra and ^{222}Rn, are retained within the parent mineral, either within the crystal lattice, or as inclusions.

In the case of the mineral uraninite, strong supporting evidence for this emerges from our own recent research on the Olympic Dam Cu–U–Au–Ag ore deposit, South Australia, where (re-)incorporation of radiogenic lead within the crystal lattice of uraninite is recognised [145–147]. Lead concentrations in Olympic Dam uraninite can, locally exceed 10 wt % in solid solution within the uraninite structure. This contradicts the findings of Janeczek and Ewing [148], where it is maintained that Pb^{2+} is incompatible within the fluorite-type uraninite structure at concentrations greater than a few wt %. Other U-minerals will also contain Pb, albeit at lower concentrations, e.g., coffinite and

brannerite from Olympic Dam [149]. Lower Pb concentrations relative to contained U suggest these structures accommodate daughter RN less well than uraninite.

The presence of radiogenic lead is also well known in minerals such as monazite and zircon where it directly substitutes into the crystal structure (e.g., [150,151]). The ratios between parent uranium, thorium and radiogenic lead underpin U–Pb geochronology. In the Olympic Dam deposit, both U and Pb (^{206}Pb) are also noted in a characteristic oscillatory-zoned textural type of hematite [152,153]. Hematite is the most abundant gangue mineral in the deposit. Within this hematite, uranium and lead isotopes, both in solid solution and as nanoparticle inclusions [154] are in apparent secular equilibrium, indicating a closed system and providing a basis for U–Pb geochronology using hematite [152,155,156].

4.2. Migration and Precipitation as New Minerals

During radioactive decay of U-bearing minerals, metamictisation will take place. This is a natural process occurring over geological time (millions to billions of years) in which the crystal structure of the parent mineral is gradually, and ultimately completely, destroyed, rendering that mineral amorphous [157]. During that process, any impurities may be expelled from the metamict phase. Even if a portion of the ^{210}Pb and ^{210}Po is retained within the U-bearing parent mineral, migration of daughter isotopes and other trace elements initially incorporated within the parent mineral (Th, REE, Nb, etc.) is widely observed to take place following metamictisation, alteration and recrystallization. The radionuclides are either precipitated as new minerals, or alternatively, are incorporated into other existing minerals at distances ranging from microns to metres from the parent phase. Such phenomena are particularly common in hydrothermal ores, in which transport is assisted by permeability and the presence of fluids. There thus exist several potential mineral hosts for daughter RN. Obvious products resulting from ^{210}Pb and ^{210}Po migration include the common lead mineral, galena, which is often observed within, or immediately adjacent to parent U-minerals ([158,159], and many others). For example, nanometre-scale galena is documented within uraninite in parts of grains in which Cu-sulphides and fluorite fill sub-micron-scale fractures [145]. Finch and Murakami [160] have outlined how galena will form in close association with uraninite if the sulphur activity is high enough. Direct evidence for the presence of ^{210}Pb within galena is limited but has been shown within recently formed galena from burning heaps associated with coal mining in the Lower Silesian basin, Czech Republic, [161]. Migrating radiogenic lead may also combine with Se or Te, either within existing minerals or from fluid, to form clausthalite (PbSe) or altaite (PbTe). Owen et al. [162] have recently documented the formation of ^{206}Pb-enriched nanoscale inclusions of clausthalite in Cu–(Fe)-sulphides, which formed via interaction between migrating Pb in fluids with Se initially hosted in solid solution within the sulphides. These may be as small as 1–2 nm in size but display coarsening.

Rollog et al. [163] have used nanoSIMS mapping to directly observe the sub-micron-scale distributions of ^{210}RN in copper ores and flotation concentrates from Olympic Dam; measurements are the sum of ^{210}Po + ^{210}Bi + ^{210}Pb but are overwhelmingly dominated by ^{210}Pb. Although concentrated within U-bearing minerals, migration of ^{210}RN away from the parent is observed on the scale of microns, with formation of nanoinclusions of "new" phases at sulphide grain boundaries, within microfractures, and within micropores in a range of host minerals. This phenomenon leads to daughter ^{210}RN becoming readily trapped within their host phases and accompanying those hosts through processing. Figure 3 shows an example of this innovative method to visualise RN distributions within individual mineral grains.

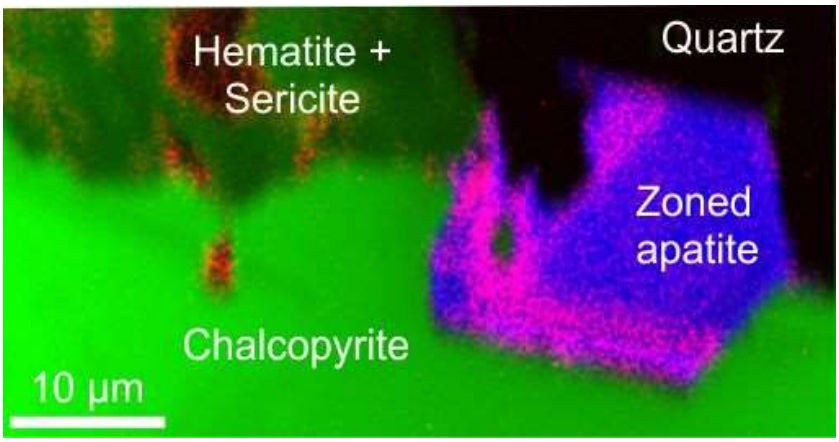

Figure 3. nanoSIMS map, modified from Rollog et al. [163] confirming the presence of ^{210}RN in apatite that is compositionally-zoned with respect to REE. Green = Fe, blue = Ca, pink = ^{210}RN.

4.3. Sulphates, Carbonates, and Other Potential Hosts

Sulphates, notably barite ($BaSO_4$), celestine ($SrSO_4$), anglesite ($PbSO_4$) and gypsum are commonly considered as hosts for radium and subsequent daughter radionuclides including ^{210}Pb and ^{210}Po. Prieto et al. [164] provide compelling experimental evidence for $(Ba,Pb)SO_4$ solid solution. We are nevertheless unaware of empirical proof for the presence of ^{210}Pb and ^{210}Po in these sulphates.

The similarity in chemical behaviour between Ra and Ba, and to some extent also Pb, makes sulphates a good host for ^{210}Pb and, potentially, for ^{210}Po. For example, Al Attar et al. [114] report barite-strontianite solid solution and *hokutolite* $[(Ba,Pb)SO_4]$ as the main mineral components of radionuclide-containing scales associated with oil production. Extensive solid solution between isostructural Ba- and Ra-sulphates (so called *radiobarite*, $(Ba,Ra)SO_4$ [165–174] has been modelled, and a number of natural occurrences have been documented e.g., [175,176]. In a detailed mineralogical insight into radionuclide host phases, Landa and Bush [79] document intense alpha particle activity associated with the presence of ^{210}Pb within micron-scale inclusions of anglesite within laths of gypsum.

Other possible candidates as hosts for ^{210}Pb and ^{210}Po in natural samples include common carbonates, notably the Pb-carbonate cerussite ($PbCO_3$). Reactions of dissolved Ra and Ba onto the surfaces of different carbonate minerals were examined by Jones et al. [177]. Calcite, dolomite, strontianite, rhodochrosite, ankerite and witherite all showed evidence of a co-precipitation reaction (increased uptake with increasing Ra concentration), siderite, magnesite and ankerite demonstrated a behaviour suggesting simple sorption. Magnesite showed a particularly high sorption capacity. An extensive treatment of the principles and mechanisms of co-precipitation with application to radionuclide incorporation within, and onto carbonate substrates, is given by Curti [178].

The role played by tellurium-bearing minerals, notably altaite (PbTe) and bismuth tellurides, as hosts for ^{210}Pb and/or ^{210}Po is unknown at the present time. These phases, as well as the selenide analogue of galena, clausthalite (PbSe) are minor yet persistent components of many hydrothermal ores, could potentially be important carriers of either radionuclide, especially given the similar chemistry of Po and Te. The environmental geochemistry of tellurium itself is only recently beginning to become better understood [179]. There may be a number of less obvious candidate hosts for ^{210}Pb and ^{210}Po. We can reasonably speculate that these will include those minerals capable of trapping gaseous radon within pore spaces during, or subsequent to growth.

4.4. Clay Minerals, Iron-Manganese-Oxides and Organics

Clay minerals, Fe–Mn oxy-hydroxides, and organic matter are well known sorbants for dissolved uranium and radium. ^{210}Pb and ^{210}Po sorption may not be primary and abundances may relate to

in-situ decay of the sorbed U and Ra. As an alternative, sorption of ^{222}Rn daughter isotopes, including ^{210}Po and ^{210}Pb may follow their generation via decay of dissolved ^{222}Rn.

In a study of a range of sites on the River Danube, preferential accumulation of ^{210}Po in sediments that are rich in clay minerals has been shown [180]. These authors invoked the ion exchange and adsorption characteristics of different types of clay minerals, suggesting that they may represent both a sink or a source for ^{210}Pb and ^{210}Po and other contaminants, as element mobilities are influenced by evolving physical, chemical and biological conditions.

A strong association between ^{210}Po and ^{210}Pb and iron oxide minerals is demonstrated in beach sands [181], even if other, far more voluminous hosts contained the majority of these and other radionuclides. Yang et al. [182] report on the adsorption properties of ^{210}Po and ^{210}Pb onto micro-particles and reported that Fe- and Mn-oxides were stronger sorbents of ^{210}Po and ^{210}Pb than SiO_2 and $CaCO_3$. They did, however, note preferential adsorption of ^{210}Po over ^{210}Pb onto both SiO_2 and $CaCO_3$. In the presence of the protein BSA; acid polysaccharides appeared to produce the opposite effect, enhancing ^{210}Pb adsorption.

Interaction, by both adsorption and incorporation, between Pb and Fe(III) (oxyhydr) oxide minerals, has been demonstrated by Yang et al. [183], who considered that the presence or absence of these minerals plays a major influence on the partitioning and transport of lead. They have shown how Pb is both surface-adsorbed and incorporated within ferrihydrite during crystallisation to hematite and goethite, depending on pH conditions.

Further evidence for the importance of both organic compounds and nanoparticles is given by Yang et al. [184], who have documented adsorption and fractionation of ^{210}Po and ^{210}Pb onto chemically simple oxide and carbonate nanoparticles in the presence or absence of various macromolecular organic compounds (MOCs) in natural seawater. MOCs were found to enhance sorption of selected nuclides on most nanoparticles (partition coefficients for ^{210}Po and ^{210}Pb increasing 2.9- and 5-fold, respectively), even if adsorption was largely dependent on particle composition.

In soils, ^{210}Po is adsorbed onto clay particles and organic material [9,185]. Sequential leaching techniques enable insights into the speciation of ^{210}Pb and ^{210}Po in soils to be gained [46]. Of the five fractions into which ^{210}Pb and ^{210}Po were fractionated, they found the majority of both ^{210}Pb (67.2%) and ^{210}Po (77.4%) bound to the insoluble residue. Small, but still significant fractions of the total ^{210}Pb (14.3%) and ^{210}Po (21.0%) were extracted with $NH_2OH{\cdot}HCl$ in 25% v/v acetic acid, which may indicate partial association of the radionuclides with Fe–Mn-oxides [186]. The bio-reactivity of ^{210}Pb and ^{210}Po was demonstrated by Kim and Kim [187], who asserted that colloids play a major role in their cycling within oceans.

Further supporting evidence for the affinity of ^{210}Pb and ^{210}Po for Fe-oxides comes from the Talvivaara mine, Eastern Finland, where microbe-induced heap leaching is used to recover Ni and by-product Zn, Cu, Co from a black schist [188,189]. Non-target metals in the deposit include uranium (as uraninite) and its daughter isotopes. The behaviour of ^{226}Ra, ^{210}Pb and ^{210}Po were studied in the mining process. It was found that they mostly remain in the heaps during leaching, where they are associated with jarosite, goethite and gypsum.

5. Discussion

5.1. Geochemical Behaviour of Daughter Radionuclides

Considerations of the likely mineral hosts for ^{210}Pb and ^{210}Po needs to include not only the geochemistry of each specific radionuclide, but the geochemical behaviour of the entire ^{238}U decay chain in the context of half-lives that range from fractions of a seconds (^{214}Po) to billions of years (^{238}U 4.5×10^9 years). The geochemical behaviours of each daughter radionuclide differ fundamentally from those of parent uranium, and thus, if released from the parent mineral and able to migrate, even if only at the sub-micron-scale, they will be readily incorporated, by virtue of ionic size and/or charge, into quite different minerals. They may potentially even undergo several "metamorphoses" before

accumulation of stable radiogenic lead within minerals such as galena or clausthalite that which do not necessarily coexist with the parent phases. Geochemical differences are particularly pronounced between U and Th, between Th and Ra, between Ra and Rn, and between Rn and Pb [2]. Figure 4 is a schematic diagram that attempts to illustrate how RN behaviour in different minerals may be viewed, also indicating how decoupling of RN within the decay chain might be achieved.

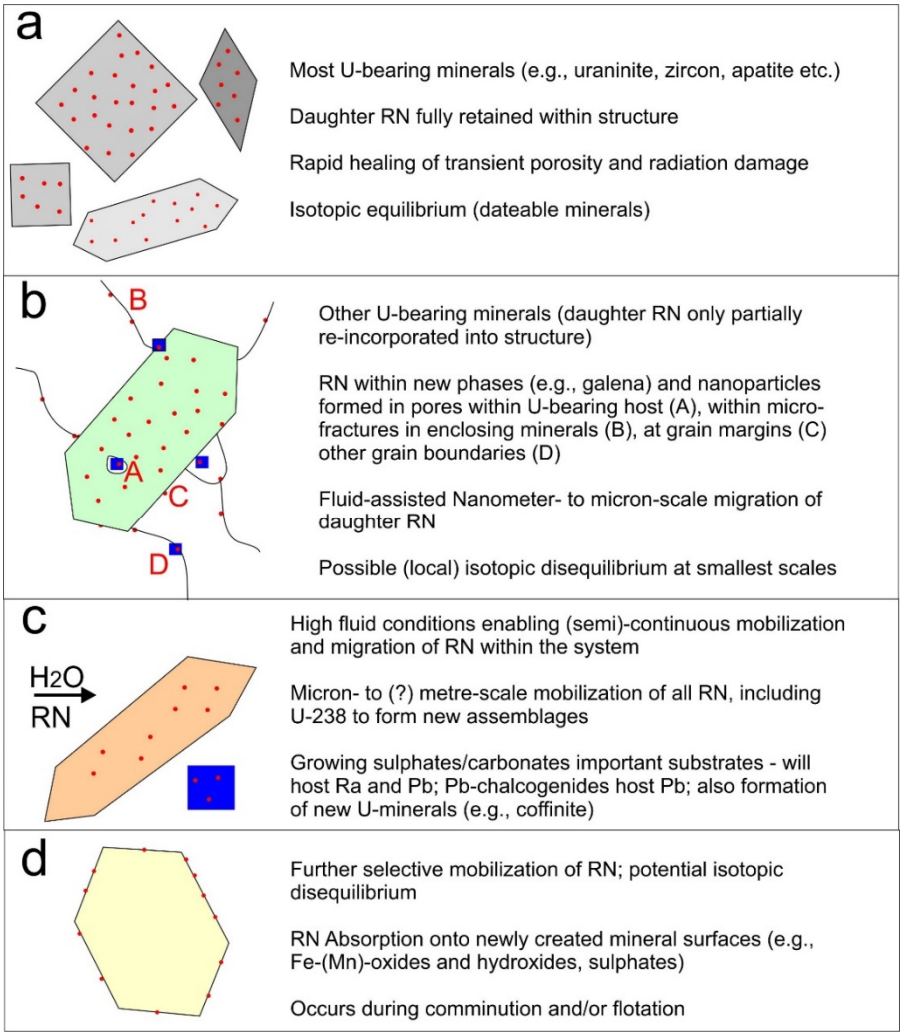

Figure 4. Schematic illustration of RN (red dots) behaviour in selected minerals within a mineralized rock, including reincorporation into parent mineral (**a**); grain-scale migration of daughter RN (**b**); fluid-assisted migration to be incorporated into new minerals (**c**) and potential adsorption of decoupled species (**d**).

Uranium can form a great variety of stable phases with different ligands. No less than 262 different uranium minerals are currently recognised, one of the largest numbers for any element in the periodic table [190]. Uranium thus belongs among a small group of elements whose mineralogical diversity is anomalous compared to its low crustal abundance. The unusual mineralogical behaviour of uranium is attributable to the unique combination of relatively large-size, high-valence and unusual coordination geometry displayed by the U^{6+} ion [191]. The hexavalent oxidation state is dominant in most U-minerals although U occurs in the tetravalent state in the most common minerals, including uraninite. Uranium mineral diversity has been amplified by Earth evolution over time with respect to oxidation state [192]. Although U^{4+} is not especially mobile, U^{6+} is highly mobile under oxidising conditions when it will readily dissolve, re-precipitating upon contact with reductants such as

sulphides or graphite. Certain minerals containing uranium undergo a process of structural breakdown (metamictisation), during which daughter radionuclides are not normally captured within the host lattice but rather migrate within or outside the mineral (e.g., [157]). In the case of uraninite, rapid annealing kinetics (e.g., [145,193]), do, however, allow for repair of radiation damage, allowing for sustained inclusion of decay product radionuclides in the mineral.

A good example of how daughter products differ geochemically from their parents is the ability for radium (^{226}Ra), unlike U or Th, to be readily enriched in the common Ba-sulphate mineral, barite. This, as examined above, takes place via direct ionic substitution (Ra^{2+} for Ba^{2+}) due to its comparable geochemical behaviour to barium with respect to charge, electronegativity and ionic size (0.143 and 0.134 nm for Ra and Ba, respectively). Although less well constrained, the potential incorporation of ^{210}Pb into galena and other Pb-bearing minerals, and of ^{210}Bi and ^{210}Po into bismuth minerals (including tellurides and other chalcogenides) may be viewed in the same way.

Decay of ^{226}Ra involves production of ^{222}Rn, a gas, which will seek to escape from the host mineral. Malczewski and Malczewski [194] have provided empirical data on ^{222}Rn and ^{220}Rn emanations from a range of metamict oxides, phosphates and silicates. These data demonstrate exponential differences in emanation rates among common minerals. Moreover, these rates vary as a function of many factors [195] closely linked to crystal structure and placing important controls on the decoupling of post-^{222}Rn decay products from parent ^{238}U. Significantly, minerals with the highest ^{238}U concentrations, notably uraninite and brannerite, showed some of the lowest ^{222}Rn and ^{220}Rn emanation coefficients. We believe that these rates—which are closely linked to crystal structure—place important controls on the decoupling of post-^{222}Rn daughter isotopes, including ^{210}Po and ^{210}Pb, from parent ^{238}U. This decoupling is expressed as secular disequilibrium on the small scale yet may not be noticed in bulk samples, or on the scale of a mineral deposit. The importance of the "radon stage" is illustrated in detailed mineralogical-isotopic study on a weathered aplite dyke [196], which showed significant (>40%) release of radon, leading to significant differences in the absolute concentrations of distributions of pre-Ra and post-Ra radionuclides.

Several studies cited in this review have given compelling evidence that particles of, or containing, ^{210}Pb and ^{210}Po are readily adsorbed onto the surfaces of clay minerals, Fe-oxides, and potentially also other minerals that can readily adsorb heavy atoms. This raises the possibility that the two radionuclides may not necessarily occur within the crystal structures of mineral phases. Evidence from disparate sources suggests that any study addressing the mineralogical deportment of ^{210}Po and ^{210}Pb must also consider that these radionuclides, or at least a significant part thereof, may not be hosted within minerals at all, but largely as nanoparticles of unknown speciation, which are adsorbed onto the surface of other minerals, such as clays, and probably, Fe-(hydr)oxides. In solid rocks, such nanoparticles may be present within micro-fractures in minerals and/or at the interfaces of mineral grains. We also believe that the affinity of ^{210}Po and ^{210}Pb for organic matter, and the potential role of organic complexes in the transport and sequestration of ^{210}Pb and ^{210}Po (e.g., biopolymers [197], should also be taken into consideration in any effort to derive a quantitative mineralogical balance for ^{210}Pb and ^{210}Po.

The physical process involved in radionuclide decay has profound consequences for understanding the mineralogical location of each daughter radionuclide. An alpha particle comprises two protons and two neutrons, the nucleus of a helium atom. When alpha decay takes place, the energy of the nucleus recoiling from alpha decay is sufficient to break chemical bonds [198], and the newly-formed nucleus (with new geochemical behaviour) will be deposited at a different site in the damaged crystal. This new position and matrix damage may make the nucleus more vulnerable to mobilisation or leaching [2]. A newly-formed radionuclide may thus migrate and be incorporated into another mineral, although this may be limited if the half-life is short, e.g., for ^{222}Rn (3.83 days) or ^{210}Bi (5 days). Cowart and Burnett [2], citing Reference [199], also make the valuable point that, if sited close to a grain boundary, the resulting nucleus may be recoiled across the grain boundary and end up in an entirely different matrix.

Roudil et al. [200] explored the creation of "bubbles" in uranium minerals from production of radiogenic helium as a product of alpha decay. This He may be concentrated in the mineral grains, or trapped at grain boundaries, also generating matrix damage. Their measurements of He outgassing from a uranium ore showed that less than 5% of the He produced was conserved, and that one-third of the residual He is occluded in the matrix and vacancy defects, and two-thirds occurred as bubbles observable by high-resolution transmission electron microscopy.

5.2. Research Trends and Future Directions

A large part of the existing literature on ^{210}Pb and ^{210}Po and their distributions in rocks and minerals concerns radioactive contamination resulting from nuclear weapons testing, uranium mining, energy generation and industrial production of fertilisers and other products from materials containing RN. These issues remain serious but have attracted markedly less research attention in the 21st century literature as industrial practices have improved. This has been compounded no doubt by the relatively short half-lives of ^{210}Pb and ^{210}Po such that their concentrations, in at least some materials produced by human activity in the past, have declined to safer levels. The contemporary literature also reflects the many ways in which radioactive waste can be efficiently treated and immobilised ([201] and references therein). Indeed, the "benefits" of man-made contamination have been highlighted in the more recent literature, notably the potential of short-lived anthropogenic radionuclides, including ^{210}Pb and ^{210}Po, as geochemical tracers for understanding processes and rates of sedimentation (e.g., [67]).

The toxicological risks from exposure to ^{210}Pb and ^{210}Po in materials from a wide range of terrestrial and marine environments are likely to remain a research focus. As older anthropogenic sources of air- and water-borne radionuclides (e.g., nuclear testing, energy generation) begin to diminish in significance, others emerge, e.g., ^{210}Po release from large-scale burning of forest biomass (e.g., [202]), or even ingestion of ^{210}Pb from calcium dietary supplements [203]. It should, however, be borne in mind that natural sources of ^{210}Pb and ^{210}Po are more significant in scale than man-made sources, e.g., from volcanic eruption. Indeed, a study of radionuclide hazards in seafood from the NW Pacific fishing area contaminated following the 2011 Fukushima nuclear accident [204] showed that despite elevated Fukushima-derived ^{90}Sr, ^{134}Cs and ^{137}Cs, these were exponentially subordinate in dose terms to natural ^{210}Pb and ^{210}Po in the same ocean area.

Despite the relative slowdown in the construction of nuclear power stations in the aftermath of the Fukushima nuclear accident, production of uranium for power generation continues to increase. Nuclear power is currently advanced as a possible low-carbon emission "green" energy alternative among the conservationist movement (e.g., [205]). In the absence of available technology to process thorium (a potential alternative fuel; [206]), increased demand necessitates a continued supply of uranium, and inevitably, as for other commodities, a need to exploit lower-grade resources, and to optimise extraction from deposits in which uranium occurs alongside other metals, notably copper, as in giant iron-oxide copper gold deposits such as Olympic Dam, South Australia.

6. Conclusions

This review has highlighted some of the many advances made in understanding the distribution of radionuclides in the environment during the past three decades. It also highlights that although the deportment and behaviour of ^{210}Pb and ^{210}Po at the scale of individual minerals is reasonably well understood, or at least predictable to some degree, there remains a paucity of direct observational data at the nano- to micron-scales to support these models. This is particularly true for metal ores and the products of their processing, for which there is an outstanding gap in knowledge. Bridging this gap is essential for generation of clean concentrates from a range of uranium-bearing ores.

Characterisation of short half-life radionuclides down to the atomic scale is now possible via use of a combination of nanoscale techniques: nanoSIMS isotope mapping [163]; scanning transmission electron microscopy with electron energy-loss spectroscopy (e.g., [207]); and high angle annular dark-field scanning transmission electron microscopy on foils prepared in-situ using focused ion

beam methods (e.g., [162,208,209]). Valuable additional constraints on RN deportment may also come from the application of nanoscale analysis techniques to radioisotope dating of minerals within hydrothermal mineral deposits forming on the present-day seafloor [210,211]. Despite these crucial advances, a fully quantitative understanding of the physical form of ^{210}Pb and ^{210}Po, and the quantitative mineral deportment of these RN in solid media, remains elusive. Researchers can, however, expect to respond to these outstanding challenges by capitalising on micro-/nanoanalytical technology, which is rapidly advancing in terms of both spatial resolution and analytical sensitivity. This will enable reliable, predictive information on the physical state of ^{210}Pb, ^{210}Po and other RN to be communicated to stakeholders, including mining companies and environmental authorities.

Author Contributions: N.J.C. conceived and coordinated this contribution. He wrote the paper in collaboration with K.J.E. and C.L.C. All other authors (M.R., D.J.L., D.S.S., N.D.O., T.H and S.R.G.) contributed otherwise unpublished data, literature and valuable discussion.

Acknowledgments: This research is a contribution to the ARC Research Hub on Australian Copper-Uranium (project number: IH130200033), funded by the Australian Research Council, BHP Olympic Dam, OZ Minerals and the South Australian Department of State Development. The authors appreciate valuable comments from three *Minerals* reviewers as well as two anonymous reviewers of a previous incarnation of this text. These have helped us improve the clarity of this manuscript.

Conflicts of Interest: The authors declare no conflict of interest. The project sponsors approve publication of the manuscript.

References

1. Lehto, J.; Hou, X. *Chemistry and Analysis of Radionuclides–Laboratory Techniques and Methodology*; Wiley-VCH: Weinheim, Germany, 2011.
2. Cowart, J.B.; Burnett, W.C. The distribution of uranium and thorium decay-series radionuclides in the environment–A review. *J. Environ. Q.* **1994**, *23*, 651–662. [CrossRef]
3. Strominger, D.; Hollander, J.M.; Seaborg, G.T. Table of isotopes. *Rev. Mod. Phys.* **1958**, *30*, 585. [CrossRef]
4. Fry, C.; Thoennessen, M. Discovery of the thallium, lead, bismuth, and polonium isotopes. *At. Data Nucl. Data Tables* **2013**, *99*, 365–389. [CrossRef]
5. Harrison, J.; Leggett, R.; Lloyd, D.; Phipps, A.; Scott, B. Polonium-210 as a poison. *J. Radiol. Prot.* **2007**, *27*, 17–40. [CrossRef] [PubMed]
6. Figgins, P.E. *The Radiochemistry of Polonium. National Academy of Sciences Nuclear Science Series*; U.S. Atomic Energy Commission: Washington, DC, USA, 1961.
7. Lane, D.J.; Cook, N.J.; Grano, S.R.; Ehrig, K. Selective leaching of penalty elements from copper concentrates: A review. *Miner. Eng.* **2016**, *98*, 110–121. [CrossRef]
8. International Atomic Energy Agency (IAEA). *Regulations for the Safe Transport of Radioactive Material*; IAEA: Vienna, Austria, 2012.
9. Parfenov, Y.D. Polonium 210 in the environment and in the human organism. *At. Energy Rev.* **1974**, *12*, 75–143. [PubMed]
10. Coppin, F.; Roussel-Debet, S. Comportement du ^{210}Po en milieu terrestre: Revue bibliographique. *Radioprotection* **2004**, *39*, 39–58. [CrossRef]
11. Landa, E.R. Naturally occurring radionuclides from industrial sources: Characteristics and fate in the environment. *Radioact. Environ.* **2007**, *10*, 211–237.
12. Persson, B.R.R.; Holm, E. Polonium-210 and lead-210 in the terrestrial environment: A historical review. *J. Environ. Radioact.* **2011**, *102*, 420–429. [CrossRef] [PubMed]
13. Baskaran, M. Po-210 and Pb-210 as atmospheric tracers and global atmospheric Pb-210 fallout: A Review. *J. Environ. Radioact.* **2011**, *102*, 500–513. [CrossRef] [PubMed]
14. Shannon, L.V.; Cherry, R.D.; Orren, M.J. Polonium-210 and lead-210 in the marine environment. *Geochim. Cosmochim. Acta* **1970**, *34*, 701–711. [CrossRef]
15. Nozaki, Y.; Thomson, J.; Turekian, K.K. The distribution of ^{210}Pb and ^{210}Po in the surface waters of the Pacific Ocean. *Earth Plan. Sci. Lett.* **1976**, *32*, 304–312. [CrossRef]
16. Bacon, M.P.; Brewer, P.G.; Spencer, D.W.; Murray, J.W.; Goddard, J. Lead-210, polonium-210, manganese and iron in the Cariaco Trench. *Deep Sea Res. Part A Oceanogr. Res. Pap.* **1980**, *27*, 119–135. [CrossRef]

17. Bacon, M.P.; Huh, C.-A.; Fleer, A.P.; Deuser, W.G. Seasonality in the flux of natural radionuclides and plutonium in the deep Sargasso Sea. *Deep Sea Res. Part A Oceanogr. Res. Pap.* **1985**, *32*, 273–286. [CrossRef]
18. González-Labajo, J.; Bolívar, J.P.; García-Tenorio, R. Natural radioactivity in waters and sediments from a Spanish mining river. *Radiat. Phys. Chem.* **2001**, *61*, 643–644. [CrossRef]
19. Balistrieri, L.S.; Murray, J.W.; Paul, B. The geochemical cycling of stable Pb, ^{210}Pb, and ^{210}Po in seasonally anoxic Lake Sammamish, Washington, USA. *Geochim. Cosmochim. Acta* **1995**, *59*, 4845–4861. [CrossRef]
20. Andrews, J.N.; Ford, D.J.; Hussain, N.; Trivedi, D.; Youngman, M.J. Natural radioelement solution by circulating groundwaters in the Stripa granite. *Geochim. Cosmochim. Acta* **1989**, *53*, 1791–1802. [CrossRef]
21. Harada, K.; Burnett, W.C.; LaRock, P.A.; Cowart, J.B. Polonium in Florida groundwater and its possible relationship to the sulfur cycle and bacteria. *Geochim. Cosmochim. Acta* **1989**, *53*, 143–150. [CrossRef]
22. Lehto, J.; Kelokaski, P.; Vaaramaa, K.; Jaakkola, T. Soluble and particle-bound ^{210}Po and ^{210}Pb in groundwaters. *Radiochim. Acta* **1999**, *85*, 149–155. [CrossRef]
23. Seiler, R.L.; Stillings, L.L.; Cutler, N.; Salonen, L.; Outola, I. Biogeochemical factors affecting the presence of ^{210}Po in groundwater. *Appl. Geochem.* **2011**, *26*, 526–539. [CrossRef]
24. Ortega, X.; Vallés, I.; Serrano, I. Natural radioactivity in drinking water in Catalonia (Spain). *Environ. Int.* **1997**, *22* (Suppl. 1), S347–S354. [CrossRef]
25. Katzlberger, C.; Wallner, G.; Irlweck, K. Determination of ^{210}Pb, ^{210}Bi and ^{210}Po in natural drinking water. *J. Radioanal. Nucl. Chem.* **2001**, *249*, 191–196.
26. Skwarzec, B.; Strumińska, D.I.; Boryło, A. Radionuclides of ^{210}Po, ^{234}U and ^{238}U in drinking bottled mineral water in Poland. *J. Radioanal. Nucl. Chem.* **2003**, *256*, 361–364. [CrossRef]
27. Simon, S.L.; Ibrahim, S.A. The plant/soil concentration ratio for calcium, radium, lead, and polonium: Evidence for non-linearity with reference to substrate concentration. *J. Environ. Radioact.* **1987**, *5*, 123–142. [CrossRef]
28. Martínez-Aguirre, A.; García-Orellana, I.; García-León, M. Transfer of natural radionuclides from soils to plants in a marsh enhanced by the operation of non-nuclear industries. *J. Environ. Radioact.* **1997**, *35*, 149–171. [CrossRef]
29. Malczewski, D.; Źaba, J. ^{222}Rn and ^{220}Rn concentrations in soil gas of Karkonosze-Izera Block (Sudetes, Poland). *J. Environ. Radioact.* **2007**, *92*, 144–164. [CrossRef] [PubMed]
30. Heyraud, M.; Cherry, R.D.; Oschadleus, H.-D.; Augustyn, C.J.; Cherry, M.I.; Sealy, J.C. Polonium-210 and Lead-210 in edible molluscs from near the Cape of Good Hope: Sources of variability in polonium-210 concentrations. *J. Environ. Radioact.* **1994**, *24*, 253–272. [CrossRef]
31. Thomas, P.A.; Gates, T.E. Radionuclides in the lichen-caribou-human food chain near uranium mining operations in northern Saskatchewan, Canada. *Environ. Health Perspect.* **1999**, *107*, 527–537. [CrossRef] [PubMed]
32. Carvalho, F.P. Polonium (^{210}Po) and lead (^{210}Pb) in marine organisms and their transfer in marine food chains. *J. Environ. Radioact.* **2011**, *102*, 462–472. [CrossRef] [PubMed]
33. Rosner, G.; Bunzl, K.; Hötzl, H.; Winkler, R. Low level measurements of natural radionuclides in soil samples around a coal-fired power plant. *Nucl. Instrum. Meth. Phys. Res.* **1984**, *223*, 585–589. [CrossRef]
34. Sahu, S.K.; Tiwari, M.; Bhangare, R.C.; Pandit, G.G. Enrichment and particle size dependence of polonium and other naturally occurring radionuclides in coal ash. *J. Environ. Radioact.* **2014**, *138*, 421–426. [CrossRef] [PubMed]
35. Schmidt, A.P. Lead precipitates from natural gas production installations. *J. Geochem. Explor.* **1998**, *62*, 193–200. [CrossRef]
36. Schmidt, A.P.; Hartog, F.A.; Van Os, B.J.H.; Schuiling, R.D. Production of ^{210}Pb from a Slochteren sandstone gas reservoir. *Appl. Geochem.* **2000**, *15*, 1317–1329. [CrossRef]
37. Al Attar, L.; Doubal, W.; Al Abdullah, J.; Khalily, H.; Abdul Ghani, B.; Safia, B. Characterization of NORM solid waste produced from the petroleum industry. *Environ. Tech.* **2015**, *36*, 1104–1113. [CrossRef] [PubMed]
38. Seen, A.; Townsend, A.; Atkinson, B.; Ellison, J.; Harrison, J.; Heijnis, H. Determining the history and sources of contaminants in sediments in the Tamar Estuary, Tasmania, using ^{210}Pb dating and stable Pb isotope analyses. *Environ. Chem.* **2004**, *1*, 49–54. [CrossRef]
39. Schindler, M.; Kamber, B.S. High-resolution lake sediment reconstruction of industrial impact in a world-class mining and smelting center, Sudbury, Ontario, Canada. *Appl. Geochem.* **2013**, *37*, 102–116. [CrossRef]

40. Matthews, K.M.; Kim, C.-K.; Martin, P. Determination of ^{210}Po in environmental materials: A review of analytical methodology. *Appl. Radiat. Isot.* **2007**, *65*, 267–279. [CrossRef] [PubMed]
41. Henricsson, F.; Ranebo, Y.; Holm, E.; Roos, P. Aspects on the analysis of ^{210}Po. *J. Environ. Radioact.* **2011**, *102*, 415–419. [CrossRef] [PubMed]
42. Flynn, W.W. The determination of low levels of polonium-210 in environmental materials. *Anal. Chim. Acta* **1968**, *43*, 221–227. [CrossRef]
43. Clayton, R.F.; Bradley, E.J. A cost effective method for the determination of ^{210}Po and ^{210}Pb in environmental materials. *Sci. Total Environ.* **1995**, *173–174*, 23–28. [CrossRef]
44. Jia, G.G.; Torri, G. Determination of ^{210}Pb and ^{210}Po in soil or rock samples containing refractory matrices. *Appl. Radiat. Isot.* **2007**, *65*, 1–8. [CrossRef] [PubMed]
45. Jia, G.G.; Belli, M.; Blasi, M.; Marchetti, A.; Rosamilia, S.; Sansone, U. Determination of ^{210}Pb and ^{210}Po in mineral and biological environmental samples. *J. Radioanal. Nucl. Chem.* **2001**, *247*, 491–499. [CrossRef]
46. Jia, G.G.; Belli, M.; Liu, S.; Sansone, U.; Xu, C.H.; Rosamilia, S.; Xiao, X.; Gaudino, S.; Chen, L.; Yang, H. The fractionation and determination procedures for the speciation of ^{210}Pb and ^{210}Po in soil samples. *Anal. Chim. Acta* **2006**, *562*, 51–58. [CrossRef]
47. Pud'homme, F.; Morency, M.; Freyer, K.; Weiss, H.; Bourne, J.; Daus, B.; Fontaine, D.; Mattusch, J.; Mineau, R.; Préda, M.; et al. Surfactant separation as a technique for physical and chemical characterization of ore processing residues. *Sci. Total Environ.* **1999**, *243/244*, 9–20.
48. Allard, P.; Aiuppa, A.; Bani, P.; Métrich, N.; Bertagnini, A.; Gauthier, P.-J.; Shinohara, H.; Sawyer, G.; Parello, F.; Bagnato, E.; et al. Prodigious emission rates and magma degassing budget of major, trace and radioactive volatile species from Ambrym basaltic volcano, Vanuatu island Arc. *J. Volc. Geotherm. Res.* **2016**, *322*, 119–143. [CrossRef]
49. Lambert, G.; Le Cloarec, M.-F.; Ardouin, B.; Le Roulley, J.-C. Volcanic emission of radionuclides and magma dynamics. *Earth Plan. Sci. Lett.* **1985**, *76*, 185–192. [CrossRef]
50. Gauthier, P.-J.; Le Cloarec, M.-F.; Condomines, M. Degassing processes at Stromboli volcano inferred from short-lived disequilibria (^{210}Pb–^{210}Bi–^{210}Po) in volcanic gases. *J. Volc. Geotherm. Res.* **2000**, *102*, 1–19. [CrossRef]
51. Rubin, K.H.; Macdougall, J.D.; Perfit, M.R. ^{210}Po–^{210}Pb dating of recent volcanic eruptions on the sea floor. *Nature* **1994**, *368*, 841–844. [CrossRef]
52. Le Cloarec, M.-F.; Gauthier, P.-J. Merapi Volcano, Central Java, Indonesia: A case study of radionuclide behavior in volcanic gases and its implications for magma dynamics at andesitic volcanoes. *J. Geophys. Res.* **2003**, *108*, 2243. [CrossRef]
53. Gill, J.B.; Williams, R.W. Th isotope and U-series studies of subduction-related volcanic rocks. *Geochim. Cosmochim. Acta* **1990**, *54*, 1427–1442. [CrossRef]
54. Berlo, K.; Turner, S. ^{210}Pb–^{226}Ra disequilibria in volcanic rocks. *Earth Plan. Sci. Lett.* **2010**, *296*, 155–164. [CrossRef]
55. Turner, S.; Reagan, M.; Vigier, N.; Bourdon, B. Origins of ^{210}Pb–^{226}Ra disequilibria in basalts: New insights from the 1978 Asal Rift eruption. *Geochem. Geophys. Geosyst.* **2012**, *13*, Q07002. [CrossRef]
56. Artemieva, I.M.; Thybo, H.; Jakobsen, K.; Sørensen, N.K.; Nielsen, L.S.K. Heat production in granitic rocks: Global analysis based on a new data compilation GRANITE2017. *Earth-Sci. Rev.* **2017**, *172*, 1–26. [CrossRef]
57. Le Cloarec, M.-F.; Pennisi, M.; Corazza, E.; Lambert, G. Origin of fumarolic fluids emitted from a nonerupting volcano: Radionuclide constraints at Vulcano (Aeolian Islands, Italy). *Geochim. Cosmochim. Acta* **1994**, *58*, 4401–4410. [CrossRef]
58. Voltaggio, M.; Tuccimei, P.; Branca, M.; Romoli, L. U-series disequilibrium radionuclides in sulphur incrustations from the fumarolic field of Vulcano Island. *Geochim. Cosmochim. Acta* **1998**, *62*, 2111–2127. [CrossRef]
59. Garavelli, A.; Laviano, R.; Vurro, F. Sublimate deposition from hydrothermal fluids at the Fossa crater (Vulcano, Italy). *Eur. J. Miner.* **1997**, *9*, 423–432. [CrossRef]
60. Vurro, F.; Garavelli, A.; Garbarino, C.; Moëlo, Y.; Borodaev, Y.S. Rare sulfosalts from Vulcano, Aeolian Islands, Italy. II. Mozgovaite, $PbBi_4(S,Se)_7$, a new mineral species. *Can. Miner.* **1999**, *37*, 1499–1506.
61. Borodaev, Y.S.; Garavelli, A.; Garbarino, C.; Grillo, S.M.; Mozgova, N.N.; Organova, N.I.; Trubkin, N.V.; Vurro, F. Rare sulfosalts from Vulcano, Aeolian Islands, Italy. III. Wittite and cannizzarite. *Can. Miner.* **2000**, *38*, 23–34. [CrossRef]

62. Garavelli, A.; Mozgova, N.N.; Orlandi, P.; Bonaccorsi, E.; Pinto, D.; Moëlo, Y.; Borodaev, Y.S. Rare sulfosalts from vulcano, Aeolian Islands, Italy. VI. Vurroite, $Pb_{20}Sn_2(Bi,As)_{22}S_{54}Cl_6$, a new mineral species. *Can. Miner.* **2005**, *43*, 703–711. [CrossRef]
63. Boisson, F.; Miquel, J.-C.; Cotret, O.; Fowler, S.W. ^{210}Po and ^{210}Pb cycling in a hydrothermal vent zone in the coastal Aegean Sea. *Sci. Total Environ.* **2001**, *281*, 111–119. [CrossRef]
64. Charmasson, S.; Sarradin, P.-M.; Le Faouder, A.; Agarande, M.; Loyen, J.; Desbruyères, D. High levels of natural radioactivity in biota from deep-sea hydrothermal vents: A preliminary communication. *J. Environ. Radioact.* **2009**, *100*, 522–526. [CrossRef] [PubMed]
65. Begy, R.C.; Dumitru, O.A.; Simon, H.; Steopoaie, I. An improved procedure for the determination of ^{210}Po by alpha spectrometry in sediments samples from Danube Delta. *J. Radioanal. Nucl. Chem.* **2015**, *303*, 2553–2557. [CrossRef]
66. Farmer, J.G.; MacKenzie, A.B.; Graham, M.C.; Macgregor, K.; Kirika, A. Development of recent chronologies and evaluation of temporal variations in Pb fluxes and sources in lake sediment and peat cores in a remote, highly radiogenic environment, Cairngorm Mountains, Scottish Highlands. *Geochim. Cosmochim. Acta* **2015**, *156*, 25–49. [CrossRef]
67. Franklin, R.L.; Fávaro, D.I.T.; Damatto, S.R. Trace metal and rare earth elements in a sediment profile from the Rio Grande Reservoir, São Paulo, Brazil: Determination of anthropogenic contamination, dating, and sedimentation rates. *J. Radioanal. Nucl. Chem.* **2015**, *307*, 99–110. [CrossRef]
68. Jones, P.; Maiti, K.; McManus, J. Lead-210 and Polonium-210 disequilibria in the northern Gulf of Mexico hypoxic zone. *Mar. Chem.* **2015**, *169*, 1–15. [CrossRef]
69. Swarzenski, P.W. ^{210}Pb Dating. In *Encyclopedia of Scientific Dating Methods*; Rink, W.J., Thompson, J.W., Eds.; Springer: Berlin, Germany, 2015; pp. 626–631.
70. Dahlkamp, F.J. *Uranium Ore Deposits*; Springer: Berlin, Germany, 1993; 460p.
71. Martin, A.; Mead, S.; Wade, B.O. *Nuclear Science and Technology: Materials Containing Natural Radionuclides in Enhanced Concentrations*; Final report for European Commission Directorate-General, Environment, Nuclear Safety and Civil Protection; Alan Martin Associates: Penetanguishene, ON, Canada, 1997; 104p.
72. Cooper, J.R.; Randle, K.; Sokhi, R.S. *Radioactive Releases in the Environment: Impact and Assessment*; John Wiley and Sons: Hoboken, NJ, USA, 2003; 773p.
73. Cooper, M.B. *Naturally Occurring Radioactive Materials (NORM) in Australian Industries–Review of Current Inventories and Future Generation: A Report Prepared for the Radiation Health and Safety Advisory Council*; EnviroRad Services Pty. Ltd.: Beaumaris, Austrilia, 2005; 40p.
74. García-Tenorio, R. ^{210}Po and ^{210}Pb in NORM mineral processing industries. In Proceedings of the EU-NORM 1st International Symposium, Tallinn, Estonia, 5–8 June 2012; pp. 202–209.
75. Xhixha, G.; Bezzon, G.P.; Broggini, C.; Buso, G.P.; Caciolli, A.; Callegari, I.; De Bianchi, S.; Fiorentini, G.; Guastaldi, E.; Kaçeli Xhixha, M.; et al. The worldwide NORM production and a fully automated gamma-ray spectrometer for their characterization. *J. Radioanal. Nucl. Chem.* **2013**, *295*, 445–457. [CrossRef]
76. Fernandes, H.M.; Franklin, M.R.; Veiga, L.H.S.; Freitas, P.; Gomiero, L.A. Management of uranium mill tailing: Geochemical processes and radiological risk assessment. *J. Environ. Radioact.* **1996**, *30*, 69–95. [CrossRef]
77. Landa, E.R. Leaching of radionuclides from uranium ore and mill tailings. *Uranium* **1982**, *1*, 53–64.
78. Landa, E.R. Uranium mill tailings: Nuclear waste and natural laboratory for geochemical and radioecological investigations. *J. Environ. Radioact.* **2004**, *77*, 1–27. [CrossRef] [PubMed]
79. Landa, E.R.; Bush, C.A. Geochemical hosts of solubilized radionuclides in uranium mill tailings. *Hydrometallurgy* **1990**, *24*, 361–372. [CrossRef]
80. Shearer, S.D., Jr.; Lee, G.F. Leachability of radium-226 from uranium mill solids and river sediments. *Health Phys.* **1964**, *10*, 217–227. [CrossRef] [PubMed]
81. Seeley, F.G. Problems in the separation of radium from uranium mill tailings. *Hydrometallurgy* **1977**, *2*, 249–263. [CrossRef]
82. Somot, S.; Pagel, M.; Thiry, J. Speciation of radium in uranium mill tailings from Ecarpière (Vendée, France). *Comptes Rendues Acad. Sci.* **1997**, *325*, 111–118.
83. Landa, E.R.; Stieff, L.R.; Germani, M.S.; Tanner, A.B.; Evans, J.R. Intense alpha particle emitting crystallites in uranium mill wastes. *Nucl. Geophys.* **1994**, *8*, 443–454.

84. Morrison, S.J.; Cahn, L.S. Mineralogical residence of alpha-emitting contamination and implications for mobilization from uranium mill tailings. *J. Contam. Hydrol.* **1991**, *8*, 1–21. [CrossRef]
85. Campbell, K.M.; Gallegos, T.J.; Landa, E.R. Biogeochemical aspects of uranium mineralization, mining, milling, and remediation. *Appl. Geochem.* **2015**, *57*, 206–235. [CrossRef]
86. Lawrence, C.E. Measurement of ^{222}Rn Exhalation Rates and ^{210}Pb Deposition Rates in a Tropical Environment. Unpublished Ph.D. Thesis, Queensland University of Technology, Brisbane City, Australia, 2006.
87. BHP Billiton Olympic Dam Expansion. Draft Environmental Impact Statement 2009. Appendix S. Uranium and Radiation. Available online: www.bhp.com (accessed on 10 April 2018).
88. Weiss, H.; Morency, M.; Freyer, K.; Bourne, J.; Fontaine, D.; Ghaleb, B.; Mineau, R.; Möder, M.; Morgenstern, P.; Popp, P.; et al. Physical and chemical characterization of a complexly contaminated scrubber dust–A by-product of copper smelting in Sachsen-Anhalt, Germany. *Sci. Total Environ.* **1997**, *203*, 65–78. [CrossRef]
89. Schreck, P. Flue dust from copper shale smelting in Central Germany: Environmental pollution and its prevention. In Proceedings of the International Mine Water Association Congress, Sevilla, Spain, 13–17 September 1999; pp. 163–167.
90. Freyer, K.; Morency, M.; Weiss, H.; Treutler, H.C.; Bourne, J. High-Alpha-Active Particles in Industrial and Mining Residues. In Proceedings of the 10th International Congress of the International Radiation Protection Association on Harmonization of Radiation, Human Life and the Ecosystem, Japan Health Physics Society, Tokyo, Japan, 14–19 May 2000.
91. Schubert, M.; Morgenstern, P.; Wennrich, R.; Freyer, K.; Paschke, A.; Weiss, H. The weathering behavior of complexly contaminated ore processing residues in the region of Mansfeld/Germany. *Mine Water Environ.* **2003**, *22*, 2–6. [CrossRef]
92. Schubert, M.; Osenbrück, K.; Knöller, K. Using stable and radioactive isotopes for the investigation of contaminant metal mobilization in a metal mining district. *Appl. Geochem.* **2008**, *23*, 2945–2954. [CrossRef]
93. Morency, M.; Weiss, H.; Freyer, K.; Bourne, J.; Fontaine, D.; Mineau, R.; Möder, M.; Morgenstern, P.; Popp, P.; Preda, M.; et al. Oxidation treatment of a sulphide-bearing scrubber dust from the Mansfeld Region, Germany: Organic and inorganic phase changes and multi-element partition coefficients between liquid and solid phases. *Sci. Total Environ.* **1998**, *223*, 87–97. [CrossRef]
94. Chau, N.D.; Jodłowski, P.; Kalia, S.J.; Olko, P.; Chruściel, E.; Maksymowicz, A.; Waligórski, M.; Bilski, P.; Budzanowski, M. Natural radiation and its hazard in copper ore mines in Poland. *Acta Geophys.* **2008**, *56*, 505–517. [CrossRef]
95. Hipkin, J.; Paynter, R.A. Radiation Exposures to the Workforce from Naturally Occurring Radioactivity in Industrial Processes. *Radiat. Prot. Dosim.* **1991**, *36*, 97–100. [CrossRef]
96. Harvey, M.P.; Hipkin, J.; Simmonds, J.R.; Mayall, A.; Cabianca, T.; Fayers, C.; Haslam, I. *Radiological Consequences of Waste Arising with Enhanced Natural Radioactivity Content from Special Metal and Ceramic Processes*; European Commission: Environment, Nuclear Safety and Civil Protection; European Commission: Brussels, Belgium, 1994.
97. Baxter, M.S.; MacKenzie, A.B.; East, B.W.; Scott, E.M. Natural decay series radionuclides in and around a large metal refinery. *J. Environ. Radioact.* **1996**, *32*, 115–133. [CrossRef]
98. Rutherford, P.M.; Dudas, M.J.; Samek, R.A. Environmental impacts of phosphogypsum: A review. *Sci. Total Environ.* **1994**, *149*, 1–38. [CrossRef]
99. Rutherford, P.M.; Dudas, M.J.; Arocena, J.M. Radium in phosphogypsum leachates. *J. Environ. Q.* **1995**, *24*, 307–314. [CrossRef]
100. Rutherford, P.M.; Dudas, M.J.; Arocena, J.M. Heterogeneous distribution of radionuclides, barium and strontium in phosphogypsum by-product. *Sci. Total Environ.* **1996**, *180*, 201–209. [CrossRef]
101. Poole, A.J.; Allington, D.J.; Baxter, A.J.; Young, A.K. The natural radioactivity of phosphate ore and associated waste products discharged into the eastern Irish Sea from a phosphoric acid production plant. *Sci. Total Environ.* **1995**, *173–174*, 137–149. [CrossRef]
102. Sam, A.K.; Holm, E. The natural radioactivity in phosphate deposits from Sudan. *Sci. Total Environ.* **1995**, *162*, 173–178. [CrossRef]
103. Burnett, W.C.; Schultz, M.H.; Hull, C.D. Radionuclide flow during the conversion of phosphogypsum to ammonium sulfate. *J. Environ. Radioact.* **1996**, *32*, 33–51. [CrossRef]

104. Hull, C.D.; Burnett, W.C. Radiochemistry of Florida phosphogypsum. *J. Environ. Radioact.* **1996**, *32*, 213–238. [CrossRef]
105. Travesí, A.; Gascó, C.; Pozuelo, M.; Palomares, J.; García, M.R.; Pérez del Villar, L. Distribution of natural radioactivity within an estuary affected by releases from the phosphate industry. *Stud. Environ. Sci.* **1997**, *68*, 267–279.
106. Mazzilli, B.; Palmiro, V.; Saueia, C.; Nisti, M.B. Radiochemical characterization of Brazilian phosphogypsum. *J. Environ. Radioact.* **2000**, *49*, 113–122. [CrossRef]
107. Silva, N.C.; Fernandes, E.A.N.; Ciprianai, M.; Taddei, M.H.T. The natural radioactivity of Brazilian phosphogypsum. *J. Radioanal. Nucl. Chem.* **2001**, *249*, 251–255.
108. Beddow, H.; Black, S.; Read, D. Naturally occurring radioactive material (NORM) from a former phosphoric acid processing plant. *J. Environ. Radioact.* **2006**, *86*, 289–312. [CrossRef] [PubMed]
109. Aoun, M.; El Samrani, A.G.; Lartiges, B.S.; Kazpard, V.; Saad, Z. Releases of phosphate fertilizer industry in the surrounding environment: Investigation on heavy metals and polonium-210 in soil. *J. Environ. Sci.* **2010**, *22*, 1387–1397. [CrossRef]
110. Hurst, F.J.; Arnold, W.D. A discussion of uranium control in phosphogypsum. *Hydrometallurgy* **1982**, *9*, 69–82. [CrossRef]
111. Pennders, R.M.J.; Köster, H.W.; Lembrechts, J.F. Characteristics of ^{210}Po and ^{210}Pb in effluents from phosphate-processing industries: A first orientation. *Radiat. Prot. Dosim.* **1992**, *45*, 737–740. [CrossRef]
112. International Atomic Energy Agency (IAEA). *The Extent of Environmental Contamination by Naturally Occurring Radioactive Material (NORM) and Technological Options for Mitigation*; IAEA Draft Technical Report; IAEA: Vienna, Austria, 2002.
113. Zielinski, R.A.; Budahn, J.R. Mode of occurrence and environmental mobility of oil-field radioactive material at US Geological Survey research site B, Osage-Skiatook Project, northeastern Oklahoma. *Appl. Geochem.* **2007**, *22*, 2125–2137. [CrossRef]
114. Al Attar, L.; Safia, B.; Abdul Ghani, B.; Al Abdullah, J. Recovery of NORM from scales generated by oil extraction. *J. Environ. Radioact.* **2016**, *153*, 149–155. [CrossRef] [PubMed]
115. Clarke, L.B.; Sloss, L.L. *Trace Elements–Emissions from Coal Combustion and Gasification*; IEA Coal Research: London, UK, 1992.
116. Tadmore, J. Radioactivity from coal-fired power plants: A review. *J. Environ. Radioact.* **1986**, *4*, 177–204. [CrossRef]
117. United Nations Scientific Committee on the Effects of Atomic Radiation (UNSCEAR). *Ionizing Radiation: Sources and Biological Effects*; United Nations: New York, NY, USA, 1982.
118. Coles, D.G.; Ragaini, R.C.; Ondov, J.M. Behaviour of natural radionuclides in western coal-fired power plants. *Environ. Sci. Tech.* **1978**, *12*, 442–446. [CrossRef]
119. Senior, C.L.; Helble, J.J.; Sarofim, A.F. Emissions of mercury, trace elements, and fine particles from stationary combustion sources. *Fuel Proc. Technol.* **2000**, *65–66*, 263–288. [CrossRef]
120. Roeck, D.R.; Reavey, T.C.; Hardin, J.M. Partitioning of natural radionuclides in the waste streams of coal-fired utilities. *Health Phys.* **1987**, *52*, 311–323. [CrossRef] [PubMed]
121. UNSCEAR. *Sources and Effects of Ionizing Radiation. Report to the General Assembly with Scientific Annexes*; United Nations: New York, NY, USA, 2010; Volume 1, 245p.
122. Barber, D.E.; Giorgio, H.R. Gamma-ray Activity in Bituminous, Subbituminous and Lignite Coals. *Health Phys.* **1977**, *32*, 83–88. [CrossRef] [PubMed]
123. Fardy, J.; McOrist, G.; Farrar, Y. Neutron activation analysis and radioactivity measurements of Australian coals and fly ashes. *J. Radioanal. Nucl. Chem.* **1989**, *133*, 217–226. [CrossRef]
124. Bhangare, R.; Tiwari, M.; Ajmal, P.; Sahu, S.; Pandit, G. Distribution of natural radioactivity in coal and combustion residues of thermal power plants. *J. Radioanal. Nucl. Chem.* **2014**, *300*, 17–22. [CrossRef]
125. Lauer, N.E.; Hower, J.C.; Hsu-Kim, H.; Taggart, R.K.; Vengosh, A. Naturally occurring radioactive materials in coals and coal combustion residuals in the United States. *Environ. Sci. Tech.* **2015**, *49*, 11227–11233. [CrossRef] [PubMed]
126. Zielinski, R.A.; Finkelman, R.B. Radioactive Elements in Coal and Fly Ash: Abundance, Forms and Environmental Significance. U.S. Geological Survey Fact Sheet FS-163-97; 1997; 4p. Available online: http://greenwood.cr.usgs.gov/energy/factshts/163-97/FS-163-97.html (accessed on 11 May 2018).

127. Długosz-Lisiecka, M. Excess of ^{210}polonium activity in the surface urban atmosphere. Part (1) fluctuation of the ^{210}Po excess in the air. *Environ. Sci. Process. Impacts* **2015**, *17*, 458–464.
128. Długosz-Lisiecka, M. Excess of polonium-210 activity in the surface urban atmosphere. Part 2: Origin of ^{210}Po excess. *Environ. Sci. Process. Impacts* **2015**, *17*, 465–470.
129. Häsänen, E.; Pohjola, V.; Hahkala, M.; Zilliacus, R.; Wickström, K. Emissions from power plants fuelled by peat, coal, natural gas and oil. *Sci. Total Environ.* **1986**, *54*, 29–51. [CrossRef]
130. Gallyas, M.; Török, I. Natural Radioactivity of Raw Materials and Products in the Cement Industry. *Radiat. Prot. Dosim.* **1986**, *7*, 69–71. [CrossRef]
131. Stojanovska, Z.; Nedelkovskia, D.; Ristovab, M. Natural radioactivity and human exposure by raw materials and end product from cement industry used as building materials. *Radiat. Meas.* **2010**, *45*, 969–972. [CrossRef]
132. Eštoková, A.; Palaščáková, L. Assessment of Natural Radioactivity Levels of Cements and Cement Composites in the Slovak Republic. *Int. J. Environ. Res. Public Health* **2013**, *10*, 7165–7179. [CrossRef] [PubMed]
133. Guillén, J.; Tejado, J.J.; Baeza, A.; Salas, A.; Muñoz-Muñoz, J.G. Environmental impact of a granite processing factory as source of naturally occurring radionuclides. *Appl. Geochem.* **2014**, *47*, 122–129. [CrossRef]
134. Harrison, J.; Heijnis, H.; Caprarelli, G. Historical pollution variability from abandoned mine sites, Greater Blue Mountains World Heritage Area, New South Wales, Australia. *Environ. Geol.* **2003**, *43*, 680–687.
135. Plater, A.J.; Appleby, P.G. Tidal sedimentation in the Tees estuary during the 20th century: Radionuclide and magnetic evidence of pollution and sedimentary response. *Estuar. Coast. Shelf Sci.* **2004**, *60*, 179–192. [CrossRef]
136. Le Roux, G.; Weiss, D.; Grattan, J.; Givelet, N.; Krachler, M.; Cheburkin, A.; Rausch, N.; Kober, B.; Shotyk, W. Identifying the sources and timing of ancient and medieval atmospheric lead pollution in England using a peat profile from Lindow bog, Manchester. *J. Environ. Monit.* **2004**, *6*, 502–510. [CrossRef] [PubMed]
137. Cloy, J.M.; Farmer, J.G.; Graham, M.C.; MacKenzie, A.B.; Cook, G.T. A comparison of antimony and lead profiles over the past 2500 years in Flanders Moss ombrotrophic peat bog, Scotland. *J. Environ. Monit.* **2005**, *7*, 1137–1147. [CrossRef] [PubMed]
138. Mayer, B.; Alpay, S.; Gould, W.D.; Lortie, L.; Rosa, F. The onset of anthropogenic activity recorded in lake sediments in the vicinity of the Horne smelter in Quebec, Canada: Sulfur isotope evidence. *Appl. Geochem.* **2007**, *22*, 397–414. [CrossRef]
139. Hansen, A.M. Lake sediment cores as indicators of historical metal(loid) accumulation–A case study in Mexico. *Appl. Geochem.* **2012**, *27*, 1745–1752. [CrossRef]
140. Gray, J.E.; Pribil, M.J.; Van Metre, P.C.; Borrok, D.M.; Thapalia, A. Identification of contamination in a lake sediment core using Hg and Pb isotopic compositions, Lake Ballinger, Washington, USA. *Appl. Geochem.* **2013**, *29*, 1–12. [CrossRef]
141. Weigel, F. Chemie des Poloniums. *Angew. Chem.* **1959**, *71*, 289–316. [CrossRef]
142. Bagnall, K.W. The Chemistry of Polonium. In *Advances in Inorganic Chemistry and Radiochemistry*; Academic Press: New York, NY, USA, 1962; Volume 4, pp. 197–226.
143. Golubev, V.N.; Chernyshev, I.V. Differential behavior of components of the ^{238}U-^{206}Pb and ^{235}U-^{207}Pb isotopic systems in polymineralic U ores. *Geochem. Int.* **2009**, *47*, 321–328. [CrossRef]
144. Connan, O.; Boust, D.; Billon, G.; Solier, L.; Rozet, M.; Bouderbala, S. Solid partitioning and solid-liquid distribution of ^{210}Po and ^{210}Pb in marine anoxic sediments: Roads of Cherbourg at the northwestern France. *J. Environ. Radioact.* **2009**, *100*, 905–913. [CrossRef] [PubMed]
145. Macmillan, E.; Cook, N.J.; Ehrig, K.; Ciobanu, C.L.; Pring, A. Uraninite from the Olympic Dam IOCG-U-Ag deposit: Linking textural and compositional variation to temporal evolution. *Am. Miner.* **2016**, *101*, 1295–1320. [CrossRef]
146. Macmillan, E.; Ciobanu, C.L.; Ehrig, K.; Cook, N.J.; Pring, A. Chemical zoning and lattice distortion: Uraninite from Olympic Dam, South Australia. *Am. Miner.* **2016**, *101*, 2351–2354. [CrossRef]
147. Macmillan, E.; Ciobanu, C.L.; Ehrig, K.; Cook, N.J.; Pring, A. Replacement of uraninite by bornite via coupled dissolution-reprecipitation: Evidence from texture and microstructure. *Can. Miner.* **2016**, *54*, 1369–1383. [CrossRef]
148. Janeczek, J.; Ewing, R.C. Mechanisms of lead release from uraninite in the natural fission reactors in Gabon. *Geochim. Cosmochim. Acta* **1995**, *59*, 1917–1931. [CrossRef]

149. Macmillan, E.; Cook, N.J.; Ehrig, K.; Pring, A. Chemical and textural interpretation of late-stage coffinite and brannerite from the Olympic Dam IOCG-Ag-U deposit. *Miner. Mag.* **2017**, *81*, 1323–1366. [CrossRef]
150. Utsunomiya, S.; Palenik, C.S.; Valley, J.W.; Cavosie, A.J.; Wilde, S.A.; Ewing, R.C. Nanoscale occurrence of Pb in an Archean zircon. *Geochim. Cosmochim. Acta* **2004**, *68*, 4679–4686. [CrossRef]
151. Kramers, J.; Frei, R.; Newville, M.; Kober, B.; Villa, I. On the valency state of radiogenic lead in zircon and its consequences. *Chem. Geol.* **2009**, *261*, 4–11. [CrossRef]
152. Ciobanu, C.L.; Wade, B.P.; Cook, N.J.; Schmidt Mumm, A.; Giles, D. Uranium-bearing hematite from the Olympic Dam Cu–U–Au deposit, South Australia: A geochemical tracer and reconnaissance Pb–Pb geochronometer. *Precambrian Res.* **2013**, *238*, 129–147. [CrossRef]
153. Verdugo-Ihl, M.R.; Ciobanu, C.L.; Cook, N.J.; Ehrig, K.; Courtney-Davies, L.; Gilbert, S. Textures and U–W–Sn–Mo signatures in hematite from the Cu–U–Au–Ag orebody at Olympic Dam, South Australia: Defining the archetype for IOCG deposits. *Ore Geology Reviews Ore Geol. Rev.* **2017**, *91*, 173–195. [CrossRef]
154. Cook, N.J.; Ciobanu, C.L.; Ehrig, K.; Slattery, A.; Verdugo-Ihl, M.R.; Courtney-Davies, L.; Gao, W. Advances and opportunities in ore mineralogy. *Minerals* **2017**, *7*, 233. [CrossRef]
155. Courtney-Davies, L.; Zhu, Z.Y.; Ciobanu, C.L.; Wade, B.P.; Cook, N.J.; Ehrig, K.; Cabral, A.R.; Kennedy, A. Matrix-matched iron-oxide laser ablation ICP-MS U–Pb geochronology using mixed solution standards. *Minerals* **2016**, *6*, 85. [CrossRef]
156. Apukhtina, O.B.; Kamenetsky, V.S.; Ehrig, K.; Kamenetsky, M.B.; Maas, R.; Thompson, J.; McPhie, J.; Ciobanu, C.L.; Cook, N.J. Early, deep magnetite-fluorapatite mineralization at the Olympic Dam Cu–U–Au–Ag deposit, South Australia. *Econ. Geol.* **2017**, *112*, 1531–1542. [CrossRef]
157. Ewing, R.C.; Meldrum, A.; Wang, L.M.; Wang, S.X. Radiation-Induced Amorphization. *Rev. Miner. Geochem.* **2000**, *39*, 319–361. [CrossRef]
158. Kerr, P.F. U-galena and uraninite in Bedford, New York cyrtolite. *Am. Miner.* **1935**, *20*, 443–450.
159. Trocki, L.K.; Curtis, D.B.; Gancarz, A.J.; Banar, J.C. Ages of Major Uranium Mineralization and Lead Loss in the Key Lake Uranium Deposit, Northern Saskatchewan, Canada. *Econ. Geol.* **1984**, *79*, 1378–1386. [CrossRef]
160. Finch, R.J.; Murakami, T. Systematics and paragenesis of uranium minerals. *Rev. Miner. Geochem.* **1999**, *38*, 91–179.
161. Čurda, M.; Goliáš, V.; Klementová, M.; Strnad, L.; Matěj, Z.; Škoda, R. Radiation damage in sulfides: Radioactive galena from burning heaps, after coal mining in the Lower Silesian basin (Czech Republic). *Am. Miner.* **2017**, *102*, 1788–1795. [CrossRef]
162. Owen, N.D.; Ciobanu, C.L.; Cook, N.J.; Slattery, A.; Basak, A. Nanoscale study of clausthalite-bearing symplectites in Cu-Au-(U) ores: Implications for ore genesis. *Minerals* **2018**, *8*, 67. [CrossRef]
163. Rollog, M.; Cook, N.J.; Guagliardo, P.; Kilburn, M.; Ehrig, K.; Ciobanu, C.L. NanoSIMS Mapping of ^{210}RN and ^{226}Ra in South Australian Copper Concentrates. Abstract, Goldschmidt Conference, Paris. 2017. Available online: https://goldschmidtabstracts.info/2017/3392.pdf (accessed on 9 May 2018).
164. Prieto, M.; Heberling, F.; Rodríguez-Galán, R.M.; Brandt, F. Crystallization behavior of solid solutions from aqueous solutions: An environmental perspective. *Progress Cryst. Growth Charact. Mater.* **2016**, *62*, 29–68. [CrossRef]
165. Takano, B.; Watanuki, K. Geochemical implications of the lead content of barite from various origins. *Geochem. J.* **1974**, *8*, 87–95. [CrossRef]
166. Rosenberg, Y.O.; Metz, V.; Ganor, J. Radium removal in a large scale evaporitic system. *Geochim. Cosmochim. Acta* **2013**, *103*, 121–137. [CrossRef]
167. Vinograd, V.L.; Brandt, F.; Rozov, K.; Klinkenberg, M.; Refson, K.; Winkler, B.; Bosbach, D. Solid-aqueous equilibrium in the $BaSO_4$-$RaSO_4$-H_2O system: First-principles calculations and a thermodynamic assessment. *Geochim. Cosmochim. Acta* **2013**, *122*, 398–417. [CrossRef]
168. Klinkenberg, M.; Brandt, F.; Breuer, U.; Bosbach, D. Uptake of Ra during the recrystallization of barite: A microscopic and time of flight-secondary ion mass spectrometry study. *Environ. Sci. Tech.* **2014**, *48*, 6620–6627. [CrossRef] [PubMed]
169. Brandt, F.; Curti, E.; Klinkenberg, M.; Rozov, K.; Bosbach, D. Replacement of barite by a (Ba,Ra)SO_4 solid solution at close-to-equilibrium conditions: A combined experimental and theoretical study. *Geochim. Cosmochim. Acta* **2015**, *155*, 1–15. [CrossRef]
170. Weber, J.; Barthel, J.; Klinkenberg, M.; Bosbach, D.; Kruth, M.; Brandt, F. Retention of ^{226}Ra by barite: The role of internal porosity. *Chem. Geol.* **2017**, *466*, 722–732. [CrossRef]

171. Heberling, F.; Metz, V.; Böttle, M.; Curti, E.; Geckeis, H. Barite recrystallization in the presence of 226 Ra and 133 Ba. *Geochim. Cosmochim. Acta* **2018**. [CrossRef]
172. Rosenberg, Y.O.; Sade, Z.; Ganor, J. The precipitation of gypsum, celestine, and barite and coprecipitation of radium during seawater evaporation. *Geochim. Cosmochim. Acta* **2018**, in press. [CrossRef]
173. Vinograd, V.L.; Kulik, D.A.; Brandt, F.; Klinkenberg, M.; Weber, J.; Winkler, B.; Bosbach, D. Thermodynamics of the solid solution-Aqueous solution system (Ba,Sr,Ra)SO_4 + H_2O: I. The effect of strontium content on radium uptake by barite. *Appl. Geochem.* **2018**, *89*, 59–74. [CrossRef]
174. Vinograd, V.L.; Kulik, D.A.; Brandt, F.; Klinkenberg, M.; Weber, J.; Winkler, B.; Bosbach, D. Thermodynamics of the solid solution-Aqueous solution system (Ba,Sr,Ra)SO_4 + H_2O: II. Radium retention in barite-type minerals at elevated temperatures. *Appl. Geochem.* **2017**. [CrossRef]
175. Ulrych, J.; Adamovič, J.; Žák, K.; Frána, J.; Řanda, Z.; Langrová, A.; Chvátal, M. Cenozoic "radiobarite" occurrences in the Ohře (Eger) Rift, Bohemian Massif: Mineralogical and geochemical revision. *Chemie der Erde–Geochem.* **2007**, *67*, 301–312. [CrossRef]
176. Zielinski, R.; Al-Hwaiti, M.; Budahn, J.; Ranville, J. Radionuclides, trace elements, and radium residence in phosphogypsum of Jordan. *Environ. Geochem. Health* **2011**, *33*, 149–165. [CrossRef] [PubMed]
177. Jones, M.J.; Butchins, L.J.; Charnock, J.M.; Pattrick, R.A.D.; Small, J.S.; Vaughan, D.J.; Wincott, P.L; Livens, F.R. Reactions of radium and barium with the surfaces of carbonate minerals. *Appl. Geochem.* **2011**, *26*, 1231–1238. [CrossRef]
178. Curti, E. *Coprecipitation of Radionuclides: Basic Concepts, Literature Review and First Applications*; Report 97-10; Paul Scherrer Institut: Villigen, Switzerland, 1997; 116p.
179. Belzile, N.; Chen, Y.W. Tellurium in the environment: A critical review focused on natural waters, soils, sediments and airborne particles. *Appl. Geochem.* **2015**, *63*, 83–92. [CrossRef]
180. Mihai, S.A.; Mather, J.D. Role of mineralogical structure of sediments in accumulation of radionuclides and trace elements. *J. Radioanal. Nucl. Chem.* **2003**, *256*, 425–430. [CrossRef]
181. McCubbin, D.; Leonard, K.S.; Maher, B.A.; Hamilton, E.I. Association of ^{210}Po(^{210}Pb), $^{239+240}$Pu and ^{241}Am with different mineral fractions of a beach sand at Seascale, Cumbria, UK. *Sci. Total Environ.* **2000**, *254*, 1–15. [CrossRef]
182. Yang, W.F.; Guo, L.D.; Chuang, C.Y.; Schumann, D.; Ayranov, M.; Santschi, P.H. Adsorption characteristics of ^{210}Pb, ^{210}Po and ^{7}Be onto micro-particle surfaces and the effects of macromolecular organic compounds. *Geochim. Cosmochim. Acta* **2013**, *107*, 47–64. [CrossRef]
183. Vu, H.P.; Shaw, S.; Brinza, L.; Benning, L.G. Partitioning of Pb(II) during goethite and hematite crystallization: Implications for Pb transport in natural systems. *Appl. Geochem.* **2013**, *39*, 119–128. [CrossRef]
184. Yang, W.F.; Guo, L.D.; Chuang, C.Y.; Santschi, P.H.; Schumann, D.; Ayranov, M. Influence of organic matter on the adsorption of ^{210}Pb, ^{210}Po and ^{7}Be and their fractionation on nanoparticles in seawater. *Earth Plan. Sci. Lett.* **2015**, *423*, 193–201. [CrossRef]
185. Häsänen, E. Dating of sediments based on 210 Po measurements. *Radiochem. Radioanal. Lett.* **1977**, *31*, 207–214.
186. Tessier, A.; Campbell, P.G.C.; Bisson, M. Sequential extraction procedure for the speciation of particulate trace metals. *Anal. Chem.* **1979**, *51*, 844–851. [CrossRef]
187. Kim, T.H.; Kim, G. Important role of colloids in the cycling of ^{210}Po and ^{210}Pb in the ocean: Results from the East/Japan Sea. *Geochim. Cosmochim. Acta* **2012**, *95*, 134–142. [CrossRef]
188. Tuovinen, H. Mobilization of Natural Uranium Series Radionuclides at Three Mining Sites in Finland. Doctoral Dissertation, University of Helsinki, Helsinki, Finland, 2015.
189. Tuovinen, H.; Pohjolainen, E.; Lempinen, J.; Vesterbacka, D.; Read, D.; Solatie, D.; Lehto, J. Behaviour of radionuclides during microbially-induced mining of nickel at Talvivaara, Eastern Finland. *J. Environ. Radioact.* **2016**, *151*, 105–113. [CrossRef] [PubMed]
190. Christy, A.G. Causes of anomalous mineralogical diversity in the Periodic Table. *Miner. Mag.* **2015**, *79*, 33–49. [CrossRef]
191. Burns, P.C. The crystal chemistry of uranium. In: Burns, P.C.; Finch, R., eds., Uranium: Mineralogy, Geochemistry and the Environment. *Rev. Miner.* **1999**, *38*, 23–90.
192. Hazen, R.M.; Ewing, R.C.; Sverjensky, D.A. Evolution of uranium and thorium minerals. *Am. Miner.* **2009**, *94*, 1293–1311. [CrossRef]

193. Janeczek, J.; Ewing, R.C. X-ray powder diffraction study of annealed uraninite. *J. Nucl. Mater.* **1991**, *185*, 66–77. [CrossRef]
194. Malczewski, D.; Malczewski, M. ^{222}Rn and ^{220}Rn emanations as a function of the absorbed α-doses from select metamict minerals. *Am. Miner.* **2015**, *100*, 1378–1385. [CrossRef]
195. Krupp, K.; Baskaran, M.; Brownlee, S.J. Radon emanation coefficients of several minerals: How they vary with physical and mineralogical properties. *Am. Miner.* **2017**, *102*, 1375–1383. [CrossRef]
196. Trindade, M.J.; Prudêncio, M.I.; Burbidge, C.I.; Dias, M.I.; Cardoso, G.; Marques, R.; Rocha, F. Study of an aplite dyke from the Beira uraniferous province in Fornos de Algodres area (Central Portugal): Trace elements distribution and evaluation of natural radionuclides. *Appl. Geochem.* **2014**, *44*, 111–120. [CrossRef]
197. Chuang, C.Y.; Santschi, P.H.; Ho, Y.F.; Conte, M.H.; Guo, L.D.; Schumann, D.; Ayranov, M.; Li, Y.H. Role of biopolymers as major carrier phases of Th, Pa, Pb, Po, and Be radionuclides in settling particles from the Atlantic Ocean. *Mar. Chem.* **2013**, *157*, 131–143. [CrossRef]
198. Osmond, J.K.; Cowart, J.B. The theory and uses of natural uranium isotopic variations in hydrology. *At. Energy Rev.* **1976**, *14*, 621–679.
199. Kigoshi, K. Alpha recoil thorium-234: Dissolution into water and the uranium-234/uranium-238 disequilibrium in nature. *Science* **1971**, *173*, 47–48. [CrossRef] [PubMed]
200. Roudil, D.; Bonhoure, J.; Pik, R.; Cuney, M.; Jégou, C.; Gauthier-Lafaye, F. Diffusion of radiogenic helium in natural uranium oxides. *J. Nucl. Mater.* **2008**, *378*, 70–78. [CrossRef]
201. Ewing, R.C.; Whittleston, R.A.; Yardley, B.W.D. Geological Disposal of Nuclear Waste: A Primer. *Elements* **2016**, *12*, 233–237. [CrossRef]
202. Carvalho, F.P.; Oliveira, J.M.; Malta, M. Exposure to radionuclides in smoke from vegetation fires. *Sci. Total Environ.* **2014**, *472*, 421–424. [CrossRef] [PubMed]
203. Strumińska-Parulska, D. Radiolead ^{210}Pb and ^{210}Po/^{210}Pb activity ratios in calcium supplements and the assessment of their possible dose to consumers. *J. Environ. Sci. Health Part A Toxic/Hazard. Subst. Environ. Eng.* **2016**, *51*, 851–854.
204. Povinec, P.P.; Hirose, K. Fukushima radionuclides in the NW Pacific, and assessment of doses for Japanese and world population from ingestion of seafood. *Sci. Rep.* **2015**, *5*, 9016. [CrossRef] [PubMed]
205. Brook, B.W.; Bradshaw, C.J.A. Key role for nuclear energy in global biodiversity conservation. *Conserv. Biol.* **2014**, *29*, 702–712. [CrossRef] [PubMed]
206. World Nuclear Association. Thorium. 2015. Available online: http://www.world-nuclear.org/information-library/current-and-future-generation/thorium.aspx (accessed on 24 July 2016).
207. Utsunomiya, S.; Kogawa, M.; Kamiishi, E.; Ewing, R.C. Scanning Transmission Electron Microscopy and Related Techniques for Research on Actinide and Radionuclide Nanomaterials. In *Actinide Nanoparticle Research*; Kalmykov, S.N., Denecke, M.A., Eds.; Springer: Berlin/Heidenberg, Germany, 2011; pp. 33–62.
208. Ciobanu, C.L.; Cook, N.J.; Maunders, C.; Wade, B.P.; Ehrig, K. Focused Ion Beam and Advanced Electron Microscopy for Minerals: Insights and Outlook from Bismuth Sulphosalts. *Minerals* **2016**, *6*, 112. [CrossRef]
209. Ciobanu, C.L.; Kontonikas-Charos, A.; Slattery, A.; Cook, N.J.; Ehrig, K.; Wade, B.P. Short-Range Stacking Disorder in Mixed-Layer Compounds: A HAADF STEM Study of Bastnäsite-Parisite Intergrowths. *Minerals* **2017**, *7*, 227. [CrossRef]
210. Uchida, A.; Toyoda, S.; Ishibashi, J.; Nakai, S. ^{226}Ra-^{210}Pb and ^{228}Ra-^{228}Th Dating of Barite in Submarine Hydrothermal Sulfide Deposits Collected at the Okinawa Trough and the Southern Mariana Trough. In *Subseafloor Biosphere Linked to Hydrothermal Systems*; Ishibashi, J., Okino, K., Sunamura, M., Eds.; Springer: Tokyo, Japan, 2015; pp. 607–615.
211. Ditchburn, R.G.; de Ronde, C.E.J. Evidence for Remobilization of Barite Affecting Radiometric Dating Using ^{228}Ra, ^{228}Th, and ^{226}Ra/Ba Values: Implications for the Evolution of Sea-Floor Volcanogenic Massive Sulfides. *Econ. Geol.* **2017**, *112*, 1231–1245. [CrossRef]